

國立交通大學

電子工程學系 電子研究所碩士班

碩士論文

多輸入多輸出系統之低複雜度偵測器研究



**A Study on Low-complexity Detectors in MIMO
Systems**

研究生：方自民

指導教授：簡鳳村 博士

中華民國九十七年八月



多輸入多輸出系統之低複雜度偵測器研究

A Study on Low-complexity Detectors in MIMO Systems

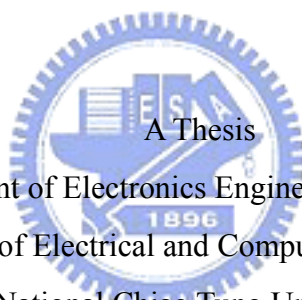
研究生：方自民

Student: Tzu-Min Fang

指導教授：簡鳳村

Advisor: Dr. Feng-Tsun Chien

國立交通大學
電子工程學系 電子研究所碩士班
碩士論文



Submitted to Department of Electronics Engineering & Institute of Electronics
College of Electrical and Computer Engineering
National Chiao Tung University
in Partial Fulfillment of the Requirements
for the Degree of Master
in
Electronics Engineering

August 2008

HsinChu, Taiwan, Republic of China

中華民國九十七年八月

多輸入多輸出系統之低複雜度偵測器研究

研究生：方自民

指導教授：簡鳳村 博士

國立交通大學

電子工程學系 電子研究所碩士班



在這篇論文我們學習 B-Chase 檢測器被應用在多輸入多輸出系統和多輸入多輸出正交分頻多工系統。B-Chase 檢測演算法是一個廣義技術它能夠提供先前所提過的檢測器當作一個特殊的實例它包含了最大概似檢測器和決策返迴檢測器。這 B-Chase 檢測器包含一個列舉檢測器，它能夠被列舉長度 l 所參數化。介由改變長度，我們能夠處理系統效能和複雜度。此外，這 B-Chase 檢測器提供兩個選擇演算法它們能夠執行一個工作去決定那一個先進來被檢測。並且列舉長度能夠影響那一個信號被第一個被檢測。這兩個選擇演算法所抉擇的信號根據兩個不同準則所決定。第一個方法是建立在接收信號的雜訊比在那裡，信號被選擇在比較高的優先權如果它有比較高的雜訊比。這個方法使得列舉檢測器的結果能夠更正確，因此下降錯誤傳送的風險。在其它方面，為了下降複雜度的需要當介由第一選擇演算法，在第二個方法執行這個選擇在這個子檢測器，能以效能去交換複雜度。最後，我們應用低複雜度 B-Chase 檢測演算法到多輸入多輸出正交分頻多工系統。

A Study on Low-complexity Detectors in MIMO Systems

Student: Tzu-Min Fang

Advisor: Dr. Feng-Tsun Chien

Department of Electronic Engineering &
Institute of Electronics
National Chiao Tung University

Abstract

We study the B-Chase detector applied to the MIMO and MIMO-OFDM systems in this thesis. B-Chase detection algorithm is a general technique that can accommodate previously reported detectors as special cases, including the maximum-likelihood and decision-feedback detectors. The B-Chase detector includes a list detector that is parameterized by the list length ℓ . By changing the list length, we can manage the system performance and complexity. In addition, the B-Chase detector provides two selection algorithms that perform the task to decide which incoming symbol is firstly detected. And the list length can impact which symbol is firstly detected. The choice of two symbol selection algorithms is determined according to two different criteria. The first approach is based on the received SNR in which the symbol is selected in a higher priority if it has a higher SNR. This way the result of the list detector is more likely to be correct, thereby reducing the risk of error propagation. On the other hand, in order to reduce the complexity entailed by the first selection algorithm, the 2nd approach performs the selection in the sub-detectors, with the performance traded to the complexity. Finally, we apply the low-complexity B-Chase algorithm to the MIMO-OFDM systems.

誌謝

要感謝我的指導教授 簡鳳村 老師,能夠讓我順利完成這篇論文。老師能夠在做研究上給予指導。感謝實驗室的其他成員和通訊電子與訊號處理實驗室(commmlab),能提供充足的軟硬體資源和幫助。這篇論文獻給所有幫助過我的人。

誌於 2008. 8 交大

自民



Contents

Chapter 1 Introduction.....	1
1.1 Significance	1
1.2 Motivation	2
1.3 Contribution.....	2
Chapter 2 MIMO Systems.....	3
2.1 Introduction to MIMO Systems.....	3
2.2 Maximum Likelihood (ML) Detection Methods.....	6
2.3 The Linear Detector Methods.....	7
2.4 BLAST Detection Methods	11
2.4.1 Combine ML and DFE Scheme	15
2.4.2 Parallel Detection (PD) Scheme	17
2.5 Chase Detector.....	21
Chapter 3 B-Chase Detector.....	25
3.1 Introduce B-Chase Detector	25
3.1.1 The SNR Gain of a List Detector for the B-Chase Detector	26
3.1.2 The SNR of the B-Chase Detector	28
3.1.3 The B-Chase Selection	30
3.1.4 Implementing the B-Chase Detector	33
3.1.5 The B-Chase Detector for Channel Estimation Errors	45
Chapter 4 B-Chase Detector of MIMO-OFDM Systems	48
4.1 OFDM System Models.....	48
4.1.1 Continuous-Time Model	49
4.1.2 Discrete-Time Model	53
4.1.3 Effect of Cyclic Prefix	54
4.2 MIMO-OFDM Architecture.....	55
4.3 B-Chase Detector in MIMO-OFDM Systems.....	57
Chapter 5 Conclusion	63

List of Figures

Figure 2-1 Model of MIMO systems	6
Figure 2-2 QR decomposition algorithm	9
Figure 2-3 Block diagram of V-BLAST structure	11
Figure 2-4 ZF V-BLAST OSIC algorithm [2]	12
Figure 2-5 The Sorted-QR decomposition algorithm [6]	14
Figure 2-6 Parallel detection.....	19
Figure 2-7 Block diagram of the Chase detector [13].....	22
Figure 3-1 Overall block diagram for the B-Chase detector	25
Figure 3-2 Decision regions for $a = e^{j\pi/4}$ and different list lengths: (a) $\ell = 1$; (b) $\ell = 2$; and (c) $\ell = 3$. The decision list contains a whenever the input to the list detector falls within the shaded region. Also indicated is the minimum distance d_ℓ to the boundary [13]	27
Figure 3-3 QR decomposition algorithm	28
Figure 3-4 Computationally efficient implementation of the B-Chase detector [13].....	36
Figure 3-5 Preprocessing pseudocode for the proposed implementation of the B-Chase detector that uses selection algorithm 1 [13]	37
Figure 3-6 The bit error rate versus SNR for the B-Chase detector* (ℓ) with $\ell=1, 2, 16$, $T=8$, and 16 QAM	40
Figure 3-7 Bit error rate versus SNR for the B-Chase detector* (ℓ) and the B-Chase detector (ℓ) with $\ell=1, 2$, $T=8$, and 16 QAM	42
Figure 3-8 Bit error rate versus SNR for the B-Chase detector* (ℓ) with $\ell=1, 2$, and the ML detector $T=8$, and BPSK.....	43
Figure 3-9 Bit error rate with channel estimation error and without channel estimation error.....	47
Figure 4-1 Cyclic prefix of an OFDM symbol [10]	49
Figure 4-2 Spectrum of an OFDM signal [10].....	52
Figure 4-3 Continuous-time OFDM baseband modulator [10]	52
Figure 4-4 Continuous-time OFDM baseband demodulator [10]	53
Figure 4-5 Discrete-time OFDM system model [10]	54
Figure 4-6 Transmitter architecture of MIMO OFDM systems	56
Figure 4-7 Receiver architecture of MIMO OFDM systems	57

Figure 4-8 Bit error rate versus SNR in the B-Chase detector* (ℓ) with $\ell=1,2,16$ for MIMO-OFDM

Systems..... 60

Figure 4-9 Bit error rate versus SNR in the B-Chase detector* (ℓ) with $\ell=1,2$ for MIMO-OFDM Systems

..... 62



List of Tables

Table 2-1 Complexity of QR decomposition algorithm	9
Table 2-2 Complexity of the Sorted-QR decomposition algorithm	14
Table 2-3 Special cases of the Chase detector [13]	23
Table 3-1 Complexity of the selection algorithm 1 and the selection algorithm 2.....	33
Table 3-2 System parameters.....	40
Table 3-3 System parameters.....	41
Table 3-4 System parameters.....	43
Table 3-5 Complexity for B-Chase Detector and ML Detector.....	44
Table 3-6 System parameters.....	46
Table 4-1 System parameters.....	59
Table 4-2 System parameters.....	61



Chapter 1

Introduction

1.1 Significance

For wireless communications applications, the major goal is to develop reliable, high data rate, and low complexity transmission systems. Therefore, future wireless communication systems are expected to provide those under all kind of channel environments, particularly with high mobility. We can realize broadband wireless systems will suffer detrimental effects of the frequency-selective fading, and many difficult engineering tasks remain to be resolved. Traditionally, getting more bandwidth is required for higher data rate transmission. However it is often impractical to increase bandwidth. Therefore, Orthogonal Frequency Division Multiplexing (OFDM) technique has received much attraction in wireless transmission applications for recent years due to the advantages to mitigate the detrimental effects of frequency-selective fading. From multiple input multiple output (MIMO) technology, we know that the rich-multipath wireless channels provide solutions to achieve spectral efficiency. In such cases, the channel between each transmit and receive antenna pair is considered flat and uncorrelated, thus Space Division Multiplexing (SDM) is a technique that can provide a significant improvement in data rate and bit error rate (BER) performance. When we employ multiple antennas at the receiver, these received data streams can be detected by SDM techniques such as Vertical–Bell Laboratories Layered Space-Time (V-BLAST) [2] [3] [8] [13]. These algorithms must require flat-fading channel information between each transmit and receive antenna pair. However, most practical channels are frequency-selective fading so that performances will be degraded. Therefore, we employ OFDM systems in which frequency-selective fading can be equivalently transformed into flat-fading in each subcarrier. In addition, it is effective when combined with SDM techniques. That is known that the SDM techniques have a performance gap for the optimal ML detectors. Hence, the goal of this research is to reduce this gap and provide new solutions to managing the inherent performance-complexity trade-off in MIMO and MIMO-OFDM detection.

1.2 Motivation

In multiple input multiple output (MIMO) technology know that the rich-multipath wireless channels between each transmit and receive antenna pair is flat and uncorrelated, thus Space Division Multiplexing (SDM) is a technique that can provide a significant improvement in data rate and bit error rate (BER) performance. Due to the SDM techniques have a performance gap for the optimal ML detectors, therefore [13] provides a total solution for managing the inherent performance-complexity trade-off in MIMO detection. The work in [13] considered flat fading channels. However, practically the channels are more likely to be frequency-selective fading. Therefore, we consider using MIMO-OFDM to tackle the problem. We aim at providing a new technique combined SDM with OFDM so that SNR as well as data rates performances can be improved.

1.3 Contribution

In this thesis, we will combine SDM and OFDM technique that can improve SNR performances as well as data rates for the practical channels are frequency-selective fading. That is shown in the chapter 4. From that we understand the system architecture is robust in the frequency-selective fading channel.

Chapter 2

MIMO Systems

The material in this Chapter is largely taken from [1], [2], [3], [4], [5], [6], [7], [8], [9], [10], [11], [12], [13], and [17].

2.1 Introduction to MIMO Systems

In wireless communication demand high data rate and high link quality access, hence we employ the multiple-input-multiple-output (MIMO) systems architectures to obtain that. We can employ different space-time code in the MIMO systems architectures to obtain high data rate and high link quality access. The high spectral efficiency due to spatial multiplex (SM), which transmit multiple data streams simultaneously by multiple antennas, and the high link quality access due to space diversity, which transmit the same multiple data streams simultaneously by multiple antennas, both at the transmitter and receiver. MIMO systems provide the ability to turn multipath propagation, which is traditionally the impairment because it can causes signal fading in the wireless transmission, into a benefit but the channel state is not correlative. Since MIMO systems effectively take advantage of random fading and multipath delay spread, the signals transmitted from each transmit antenna appear highly uncorrelated at each receive antenna and the signals travel through different spatial channels. Then the receiver can exploit these different spatial channels and separate the signals transmitted from different antennas at the same frequency band simultaneously.

MIMO is a promising technology that is suite for high-speed broadband wireless communications. Through space division multiplexing, MIMO technology can transmit multiple data streams in independent parallel spatial channels, thereby increasing total system transmission rate. Considering an arbitrary wireless communication system, a link is considered for that the transmitter is equipped with N_t transmit antennas and the receiver is equipped with N_r receive antennas. Such a setup is illustrated in Figure. 2.1. considered at some assumptions.

Consider this system some important assumptions are made first:

1. Channels are constant during the transmission of a packet. It means the communication is carried out in the some packets period that are shorter than the coherence time of the channels. The channel state is assumed that is time invariance.
2. Channels are memoryless. It means that an independent channel realization is drawn for each use of the channels.
3. The channel is flat fading. It means that constant fading over the bandwidth is desired in the case of narrowband transmissions. It also indicates that the channel gains can be described by complex numbers.
4. The received signal is corrupted by additive white Gaussian noise (AWGN).
5. At all time the receiver can perfectly know the channel matrix which is also known as the channel state information (CSI) and the CSI can be obtained by channel estimation based on the transmission of a training sequence.

With these assumptions, it is common to represent the input/output relations of a narrowband, single-user MIMO link by the complex baseband vector notation and transmit signal vector is transmitted at each instant time.

$$\mathbf{r} = \mathbf{H}\mathbf{a} + \mathbf{w} \quad (2.1.1)$$

where $\mathbf{a} = [a_1, \dots, a_{N_t}]^T$ is the $N_t \times 1$ transmitted signal vector in \mathbb{R}^{N_t} or \mathbb{C}^{N_t} whose entries are chosen from some complex constellation A (e.g. 16-QAM etc.), $\mathbf{r} \in \mathbb{C}^{N_r}$ is the received signal vector is the $N_r \times 1$ received vector, $\mathbf{H} = [\mathbf{h}_1, \dots, \mathbf{h}_{N_t}]$ is $\mathbb{C}^{N_r \times N_t}$ the Rayleigh flat fading channel matrix whose i th column is \mathbf{h}_i , and where $\mathbf{w} = [w_1, \dots, w_{N_r}]^T$ is \mathbb{C}^{N_r} zero-mean complex Gaussian noise vector at some instant time. We assume that the columns of \mathbf{H} are linearly independent (e.g. $N_r \geq N_t$). We assume that the noise components are independent and identically distributed (i.i.d.) complex Gaussian random variable with $E[\mathbf{w}\mathbf{w}^H] = N_0\mathbf{I}$

that is additive white Gaussian noise (AWGN). We assume that the complex inputs are uncorrelated and chosen from the same unit-energy discrete alphabet, so that $E[\mathbf{a}\mathbf{a}^H] = \mathbf{I}$. All the coefficients h_{ij} comprise the channel matrix \mathbf{H} and represent the complex gain of the channel between the j th transmit antenna and the i th receive antenna. The channel matrix can be written as

$$\mathbf{H} = \begin{bmatrix} h_{1,1} & h_{1,2} & \cdots & h_{1,N_t} \\ h_{2,1} & h_{2,2} & \cdots & h_{2,N_t} \\ \vdots & \vdots & \ddots & \vdots \\ h_{N_r,1} & h_{N_r,2} & \cdots & h_{N_r,N_t} \end{bmatrix} \quad (2.1.2)$$

$$h_{i,j} = \alpha_{i,j} + j\beta_{i,j} = |h_{i,j}| e^{j\phi_{i,j}} \quad (2.1.3)$$

Those coefficients $\{h_{ij}\}$ describe the unknown channel properties of the medium that is usually Rayleigh distributed in a rich scattering environment without line-of-sight (LOS) path. If α_{ij} and β_{ij} are independent and Gaussian distributed random variables, then $|h_{ij}|$ is a Rayleigh distributed random variable. Actually, those coefficients $\{h_{ij}\}$ are likely to be subject to varying degrees of fading and change over time. Therefore, determination of the channel matrix is an important and necessary aspect of MIMO techniques. If all these coefficients are known, there will be sufficient information for the receiver to eliminate interference from other transmitters operating at the same frequency band. Although the introduced MIMO transmission requires flat-fading channels, and it is limited to applications with narrowband transmissions, in real broadband transmission systems, channel conditions are often frequency-selective fading. In wireless transmission, we demand a technique to alleviate the severe effect of frequency-selective fading. Therefore the OFDM technique is a good solution for this purpose in wireless transmission owing to its advantages.

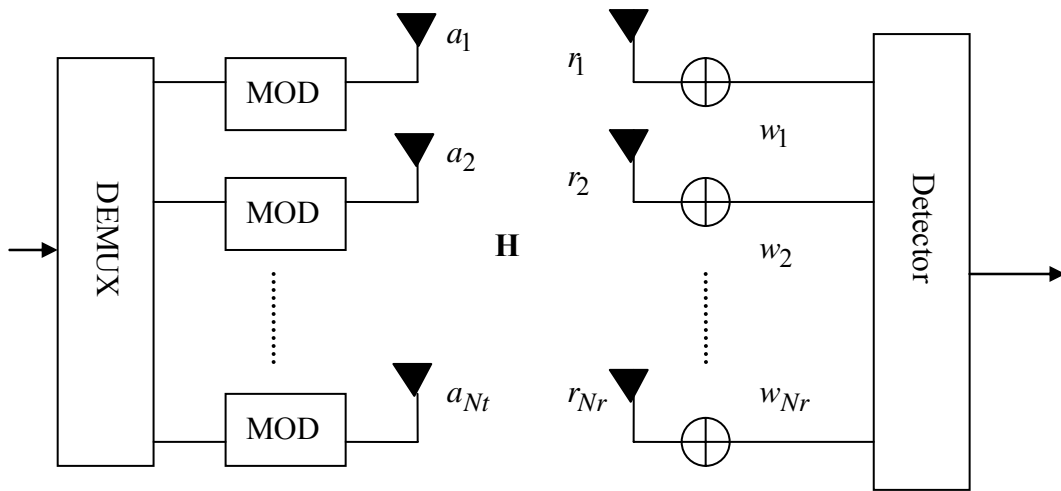


Figure 2-1 Model of MIMO systems

2.2 Maximum Likelihood (ML) Detection Methods

First, we will employ the Maximum Likelihood (ML) Detection for the MIMO systems and it is given by

$$\hat{\mathbf{a}}_{ML} = \arg \min_{\mathbf{a} \in A^{N_t}} \|\mathbf{r} - \mathbf{H}\mathbf{a}\|^2 \quad (2.2.1)$$

From the transmitted vector symbols, A is the complex-valued modulating constellation and A^{N_t} is the entire set of the possible transmitted vector symbols. We know that find the entire set of the possible transmitted vector symbols so that the complexity is huge due to N_t and A . We know that N_t is the transmit antennas and A is the complex-valued modulating constellation, so N_t and A is huge such that spend much complexity to find the solution from (2.2.1). From the optimal Maximum Likelihood (ML) Detection in the MIMO systems know the complexity increases when N_t and A increases, so find the suboptimal detection for the MIMO systems.

2.3 The Linear Detector Methods

We could employ these linear detectors for the MIMO systems. The received signal vector \mathbf{r} is multiplied with a filter matrix \mathbf{G} and then followed by a parallel decision on all layers. Zero-forcing means that the mutual interference between the layers shall be perfectly suppressed. This is accomplished by the Moore-Penrose pseudo-inverse (denoted by $(\cdot)^+$) of the channel matrix

$$\mathbf{G}_{ZF} = \mathbf{H}^+ = (\mathbf{H}^H \mathbf{H})^{-1} \mathbf{H}^H \quad (2.3.1)$$

where we assume that \mathbf{H} has full column rank. The decision step consists of mapping each element of the filter output vector

$$\bar{\mathbf{a}}_{ZF} = \mathbf{G}_{ZF} \mathbf{r} = \mathbf{a} + (\mathbf{H}^H \mathbf{H})^{-1} \mathbf{H}^H \mathbf{w} \quad (2.3.2)$$

into an element of the symbol alphabet by a minimum distance quantization. The estimation errors of the different layers correspond to the main diagonal elements of the error covariance matrix

$$\Phi_{ZF} = E\{(\bar{\mathbf{a}}_{ZF} - \mathbf{a})(\bar{\mathbf{a}}_{ZF} - \mathbf{a})^H\} = \sigma_w^2 (\mathbf{H}^H \mathbf{H})^{-1} \quad (2.3.3)$$

which equals the covariance matrix of the noise after the receive filter. It is obvious that small eigenvalues of $\mathbf{H}^H \mathbf{H}$ will lead to large errors due to noise amplification. This effect is especially observed in systems with the same number of transmit and receive antennas. We can use Linear MMSE detector to decrease the noise amplification. Minimizing the mean squared error (MSE) between the actually transmitted symbols and the output of a linear detector leads to the filter matrix

$$\mathbf{G}_{MMSE} = (\mathbf{H}^H \mathbf{H} + \sigma_w^2 \mathbf{I}_{N_t})^{-1} \mathbf{H}^H \quad (2.3.4)$$

The resulting filter output is given by

$$\bar{\mathbf{a}}_{MMSE} = \mathbf{G}_{MMSE} \mathbf{r} = (\mathbf{H}^H \mathbf{H} + \sigma_w^2 \mathbf{I}_{N_t})^{-1} \mathbf{H}^H \mathbf{r} \quad (2.3.5)$$

and, after some manipulations, the error covariance matrix is found to be

$$\Phi_{MMSE} = \sigma_w^2 (\mathbf{H}^H \mathbf{H} + \sigma_w^2 \mathbf{I}_{N_t})^{-1} \quad (2.3.6)$$

With the definition of a $(N_t+N_r) \times N_t$ extended channel matrix $\underline{\mathbf{H}}$ and a $(N_t+N_r) \times 1$ extended receive vector $\underline{\mathbf{r}}$ through

$$\underline{\mathbf{H}} = \begin{bmatrix} \mathbf{H} \\ \sigma_w \mathbf{I}_{N_t} \end{bmatrix} \quad \text{and} \quad \underline{\mathbf{r}} = \begin{bmatrix} \mathbf{r} \\ \mathbf{0}_{N_t,1} \end{bmatrix} \quad (2.3.7)$$

We can write the output of the MMSE filter as

$$\bar{\mathbf{a}}_{MMSE} = (\underline{\mathbf{H}}^H \underline{\mathbf{H}})^{-1} \underline{\mathbf{H}}^H \underline{\mathbf{r}} = \underline{\mathbf{H}}^+ \underline{\mathbf{r}} \quad (2.3.8)$$

Furthermore, the error covariance matrix becomes

$$\Phi_{MMSE} = \sigma_w^2 (\underline{\mathbf{H}}^H \underline{\mathbf{H}})^{-1} \quad (2.3.9)$$

We compare that are the corresponding expression for zero-forcing that can find the only difference is that the channel matrix \mathbf{H} has been replaced by $\underline{\mathbf{H}}$. We can use the QR

decomposition of the channel matrix for ZF or MMSE. For ZF, we can do the QR decomposition of the channel matrix $\mathbf{H}=\mathbf{Q}\mathbf{R}$ that we can rewrite the a filter matrix as

$$\mathbf{G}_{ZF} = \mathbf{H}^+ = \mathbf{R}^{-1}\mathbf{Q}^H \quad (2.3.10)$$

1. *function* $\mathbf{H} = \mathbf{Q}\mathbf{R}$
2. $\mathbf{R} = \mathbf{0}, \mathbf{Q} = [\mathbf{q}_1, \mathbf{q}_2, \dots, \mathbf{q}_{Nt}] = \mathbf{H}$
3. *for* $i = 1, \dots, Nt$
4. $r_{i,i} = |\mathbf{q}_i|$
5. $\mathbf{q}_i = \mathbf{q}_i / r_{i,i}$
6. *for* $j = i + 1, \dots, Nt$
7. $\mathbf{q}_j = \mathbf{q}_j - r_{i,j} \cdot \mathbf{q}_i$
8. *end*
9. *end*

Figure 2-2 QR decomposition algorithm

Table 2-1 Complexity of QR decomposition algorithm

	No. Multiplication	Nr=4, Nt=4
4.	Mult:2Nr	8

7.	Mult:3Nr	12
ZF total complex	Mult:2*Nr+3*Nr*(Nt) ² -3Nr*Nt	152
MMSE total complex	Mult:3(Nt) ³ -3Nr(Nt) ² -3(Nt) ² -3NrNt+2Nr+2Nt	304

For MMSE, we can do the QR decomposition of the extended channel matrix that we can write as

$$\underline{\mathbf{H}} = \begin{bmatrix} \mathbf{H} \\ \sigma_w \mathbf{I}_{N_t} \end{bmatrix} = \underline{\mathbf{Q}} \underline{\mathbf{R}} = \begin{bmatrix} \mathbf{Q}_1 \\ \mathbf{Q}_2 \end{bmatrix} \underline{\mathbf{R}} = \begin{bmatrix} \mathbf{Q}_1 \underline{\mathbf{R}} \\ \mathbf{Q}_2 \underline{\mathbf{R}} \end{bmatrix} \quad (2.3.11)$$

where the $(N_t+N_r) \times N_t$ matrix $\underline{\mathbf{Q}}$ with orthonormal columns was partitioned into the $N_r \times N_t$ matrix \mathbf{Q}_1 and the $N_t \times N_t$ matrix \mathbf{Q}_2 . From that equation we get the relation as

$$\underline{\mathbf{R}}^{-1} = \frac{1}{\sigma_w} \mathbf{Q}_2 \quad (2.3.12)$$

Furthermore,

$$\underline{\mathbf{Q}}^H \underline{\mathbf{H}} = \mathbf{Q}_1^H \mathbf{H} + \sigma_w \mathbf{Q}_2^H = \underline{\mathbf{R}} \quad (2.3.13)$$

holds. The filtered receive vector becomes

$$\tilde{\mathbf{a}} = \underline{\mathbf{Q}}^H \underline{\mathbf{r}} = \mathbf{Q}_1^H \mathbf{r} = \underline{\mathbf{R}} \mathbf{a} - \sigma_w \underline{\mathbf{R}}^{-H} \mathbf{a} + \mathbf{Q}_1^H \mathbf{w} \quad (2.3.14)$$

From the filtered receive vector we know that we have the remaining interference that can not be removed in the detected procedure.

2.4 BLAST Detection Methods

For get high data rate and performance in the MIMO systems, therefore employ Vertical – Bell Laboratories Layered Space-Time (V-BLAST) Architecture to implement that.

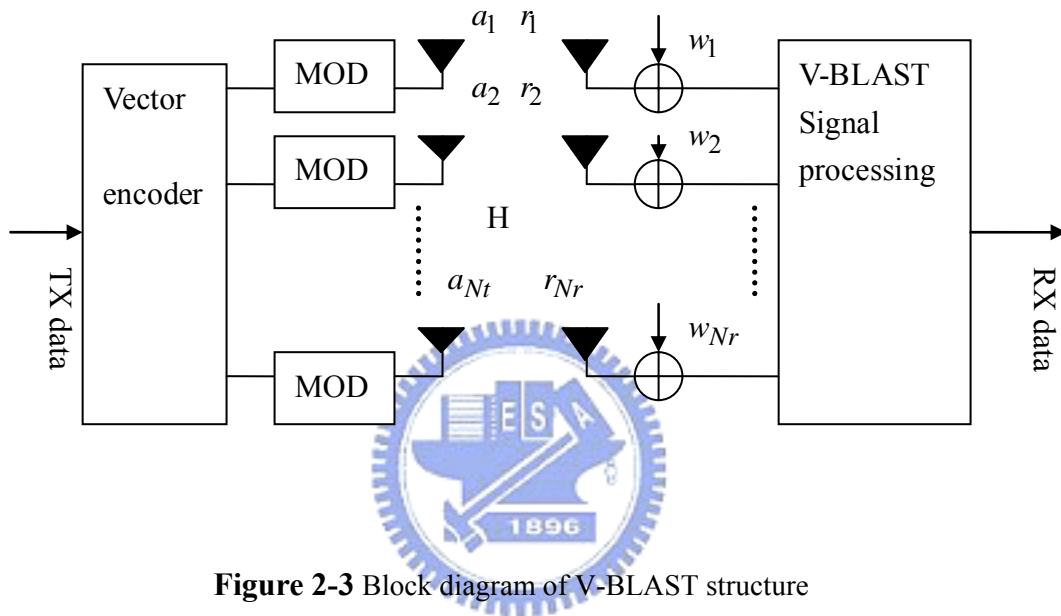


Figure 2-3 Block diagram of V-BLAST structure

Where the transmit antennas send a vector symbol of the size N_t over a rich-scattering wireless channel to the N_r receive antennas at each symbol time. At the transmitter, a single data stream is partitioned into N_t substreams, and each substream is encoded and sent through a different transmit antenna. During reception, each antenna receives signals transmitted from all the N_t transmit antennas. We are base on (V-BLAST) Architecture to find some detector. We use successive interference cancellation (SIC) technique or ordered SIC (OSIC) based on zero-forcing criterion (ZF V-BLAST) that require the decision-feedback equalization (DFE) and detect sequentially transmitted signals with the smallest estimation error. On zero-forcing criterion find the filter matrix \mathbf{G}_{ZF} . For get the smallest estimation error, so find the largest signal-to-noise ratio (SNR) and reduce noise enhancement. Find the row \mathbf{g}_{ZF} of \mathbf{G}_{ZF} that has the minimum norm and multiply the received signal.

$$\hat{a}_i = \mathbf{g}_{ZF}^i \mathbf{r} = \mathbf{g}_{ZF}^i (\mathbf{H}\mathbf{a} + \mathbf{w}) = a_i + \eta_i \quad (2.4.1)$$

where i is the order index a signal is detected. \hat{a}_i is quantized to get estimate of a_i and regenerate an estimate of signal then the received signal subtract the regenerate an estimate of signal to remove the interference of this signal. Sequential do Nulling and canceling process until all signals are detected. That is shown

```

B e g i n
H1 = H
r1 = r
f o r (i = 1; i <= Nt, i + + )
    GiZF = (Hi)+
    ki = a r g j m i n ||(GiZF)j ||
    giZF = (GiZF)ki
     $\hat{a}_i = \mathbf{g}_{ZF}^i \mathbf{r}$ 
    aki = q u a n t i z e ( $\hat{a}_i$ )
    ri+1 = ri - aki Hki
    Hi+1 = Hiki
e n d

```

Figure 2-4 ZF V-BLAST OSIC algorithm [2]

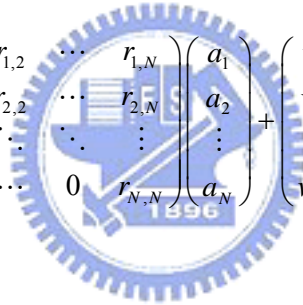
where \mathbf{g}_{ZF}^i means the k_i -th row of \mathbf{G}_{ZF}^i , \mathbf{H}_{k_i} means the k_i -th column of \mathbf{H} , and

$\mathbf{H}_{k_i}^i$ means the resulting matrix \mathbf{H} after nulling the k_i -th column of \mathbf{H}^i . To find the

ordering do the repeated computations of a channel matrix pseudoinverse and spend much complexity with $O(Nt^4)$, where Nt is the number of channel inputs. We find a low complexity algorithm to do the repeated computations of a channel matrix pseudoinverse and the ordering for the performance. We employ the decision-feedback (DF) detector that to do

nulling and canceling. We can know the risk of error propagation in the decision-feedback (DF) detector, so find out the best ordering to reduce the risk of error propagation. That is to find the max SNR at the first time which reduces the detection errors to do nulling and canceling. Find the low complexity algorithm or/and the best performance on the below when assume $N_t = N_r = N$. We will use the QR and the sorted QR decomposition in V-BLAST to reduce the complexity. Use the QR decomposition to decompose the $\mathbf{H} = \mathbf{Q}\mathbf{R}$ that \mathbf{Q} is the $N \times N$ unitary matrix and \mathbf{R} is the $N \times N$ upper triangular matrix and we know the amplitudes of the entries of the matrix \mathbf{R} are χ -distributed. We use the feedforward filter matrix \mathbf{Q}^H for the received signal. That is shown.

$$\tilde{\mathbf{r}} = \mathbf{Q}^H (\mathbf{H}\mathbf{a} + \mathbf{w}) = \mathbf{R}\mathbf{a} + \tilde{\mathbf{w}} \quad (2.4.2)$$



$$\begin{pmatrix} \tilde{r}_1 \\ \tilde{r}_2 \\ \vdots \\ \tilde{r}_N \end{pmatrix} = \begin{pmatrix} r_{1,1} & r_{1,2} & \cdots & r_{1,N} \\ 0 & r_{2,2} & \cdots & r_{2,N} \\ \vdots & \vdots & \ddots & \vdots \\ 0 & \cdots & 0 & r_{N,N} \end{pmatrix} \begin{pmatrix} a_1 \\ a_2 \\ \vdots \\ a_N \end{pmatrix} + \begin{pmatrix} \tilde{w}_1 \\ \tilde{w}_2 \\ \vdots \\ \tilde{w}_N \end{pmatrix}$$

Since \mathbf{Q} is unitary, the statistical properties of the noise term $\tilde{\mathbf{w}} = \mathbf{Q}^H \mathbf{w}$ remain unchanged. First, we can use the last row to solve the last equation and that is shown.

$$\begin{aligned} \tilde{r}_N &= r_{N,N}a_N + \tilde{w}_N && \rightarrow \text{get } \hat{a}_N \\ \tilde{r}_{N-1} &= r_{N-1,N-1}a_{N-1} + r_{N-1,N}a_N + \tilde{w}_{N-1} && \rightarrow \text{get } \hat{a}_{N-1} \\ &\vdots && \\ \tilde{r}_1 &= r_{1,1}a_1 + \sum_{j=2}^N r_{1,j}\hat{a}_j + \tilde{w}_1 && \rightarrow \text{get } \hat{a}_1 \end{aligned}$$

Form that we know the first time to solve the equation and it can affect the performance. If we can solve the equation at the first time is error then we can have much error at the second time. We call that is error propagation. So, we will use the sorted QR decomposition to choose which columns of \mathbf{H} at the first time. That can get the optimum \mathbf{R} to solve the equation. We

can use the complexity $O(N^2/2)$ in the QR decomposition of permutations of \mathbf{H} . We can use the sorted QR decomposition that use an extension of the modified Gram-Schmidt (MGS) algorithm by ordering the columns of \mathbf{H} in each orthogonalisation step. That algorithm is shown.

1. $\mathbf{R} = \mathbf{0}, \mathbf{Q} = \mathbf{H}, \mathbf{p} = (1, \dots, N)$
2. *for* $i = 1, \dots, N$
3. $k_i = \arg \min_{j=i, \dots, N} |\mathbf{q}_j|^2$
4. *exchange columns* i *and* k_i *in* $\mathbf{R}, \mathbf{Q}, \mathbf{p}$
5. $r_{i,i} = |\mathbf{q}_i|$
6. $\mathbf{q}_i = \mathbf{q}_i / r_{i,i}$
7. *for* $j = i+1, \dots, N$
8. $\mathbf{q}_j = \mathbf{q}_j - r_{i,j} \cdot \mathbf{q}_i$
9. *end*

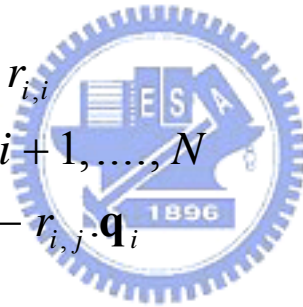


Figure 2-5 The Sorted-QR decomposition algorithm [6]

Table 2-2 Complexity of the Sorted-QR decomposition algorithm

	No. Multiplication	Nr=Nt=N=4
3.	Mult: $2N_r \cdot N_t$	32
5.	Mult: $2N_r$	8

8.	Mult:3Nr	12
ZF total complex	Mult:3.5*Nr*(Nt) ² +0.5Nr*Nt	232
MMSE total complex	Mult: 3.5*Nr*(Nt) ² +3.5(Nt) ³ +0.5Nr*Nt+0.5(Nt) ²	464

We find the permutation vector \mathbf{p} that store the used reordering of \mathbf{H} that minimises each $|r_{k,k}|$ with k running from 1 to N.. We consequently compute the diagonal elements that are calculated from $r_{1,1}$ to $r_{N,N}$ and it would be optimal to maximise the $|r_{k,k}|$ in every decoding step, that means from $r_{N,N}$ to $r_{1,1}$. That can reduce the risk of error propagation because we have the huge SNR gain in the Nth subchannel. We will know the performance is limited by the Nth subchannel. The performance of V-BLAST is limited by the worst subchannel, i.e., subchannel N. Basically this is due to the error propagation which is inherent in a DFE, and the distribution of the upper triangular matrix \mathbf{R} . The amplitudes of the entries of \mathbf{R} have x distribution with different degrees of freedom, and furthermore, $r_{N,N}$ has the least degree of freedom. Therefore, the Nth subchannel has the worst statistics, and it is crucial to improve its statistics in order to improve the overall performance of the V-BLAST. So we propose to combine ML decoding with the DFE procedure.

2.4.1 Combine ML and DFE Scheme

On the below when assume $N_t = N_r = N$. For the worst p subchannels, we perform ML decoding and then use a DFE for the remaining subchannels. In order to do this, we do not completely triangularize the channel matrix \mathbf{H} . That is shown.

$$\mathbf{H} = \tilde{\mathbf{Q}} \begin{pmatrix} \tilde{\mathbf{R}} & \mathbf{H}_a \\ \mathbf{0} & \mathbf{H}_b \end{pmatrix} \quad (2.4.1.1)$$

where $\tilde{\mathbf{R}}$ is an upper triangular matrix of size $(N-p) \times (N-p)$ and \mathbf{H}_b is a square matrix of size $p \times p$. To get the above decomposition, we follow the usual Gram-Schmidt orthogonalization procedure for $(\underline{\mathbf{h}}_1, \underline{\mathbf{h}}_2, \dots, \underline{\mathbf{h}}_{N-p})$ which yields

$$\mathbf{H} = (\tilde{\mathbf{Q}}_a \tilde{\mathbf{R}} | \underline{\mathbf{h}}_{N-p+1}, \underline{\mathbf{h}}_{N-p+2}, \dots, \underline{\mathbf{h}}_N) \quad (2.4.1.2)$$

where $\underline{\mathbf{h}}_j$ is the j th column of \mathbf{H} . Now we find an arbitrary $\tilde{\mathbf{Q}}_b$ of size $N \times p$ such that $\tilde{\mathbf{Q}}_b^H \tilde{\mathbf{Q}}_b = \mathbf{I}$ and $\tilde{\mathbf{Q}}_b^H \tilde{\mathbf{Q}}_a = \mathbf{0}$. Thus $\tilde{\mathbf{Q}} = (\tilde{\mathbf{Q}}_a | \tilde{\mathbf{Q}}_b)$ form an orthonormal basis. Then choose \mathbf{H}_a and \mathbf{H}_b such that

$$(\tilde{\mathbf{Q}}_a \tilde{\mathbf{Q}}_b) \begin{pmatrix} \mathbf{H}_a \\ \mathbf{H}_b \end{pmatrix} = (\underline{\mathbf{h}}_{N-p+1}, \underline{\mathbf{h}}_{N-p+2}, \dots, \underline{\mathbf{h}}_N) \quad (2.4.1.3)$$

Since $\tilde{\mathbf{Q}}_b$ is independent of $(\underline{\mathbf{h}}_{N-p+1}, \underline{\mathbf{h}}_{N-p+2}, \dots, \underline{\mathbf{h}}_N)$, the elements of \mathbf{H}_b are i.i.d. complex Gaussian with zero mean and unit variance. Using this decomposition, we first detect $(a_{N-p+1}, a_{N-p+2}, \dots, a_N)^T$ jointly by ML decoding of size p , cancel the interferences caused by these symbols, and then detect $(a_1, a_2, \dots, a_{N-p})^T$ by the usual DFE procedure. For the decomposition of \mathbf{H} we use that for the received signal and show that.

$$\begin{aligned} \tilde{\mathbf{r}} &= \tilde{\mathbf{Q}}^H \mathbf{r} \\ \begin{pmatrix} \tilde{\mathbf{r}}_a \\ \tilde{\mathbf{r}}_b \end{pmatrix} &= \begin{pmatrix} \tilde{\mathbf{R}} & \mathbf{H}_a \\ \mathbf{0} & \mathbf{H}_b \end{pmatrix} \begin{pmatrix} \mathbf{a}_a \\ \mathbf{a}_b \end{pmatrix} + \begin{pmatrix} \mathbf{w}_a \\ \mathbf{w}_b \end{pmatrix} \end{aligned} \quad (2.4.1.4)$$

We perform ML decoding with $\tilde{\mathbf{r}}_b = \mathbf{H}_b \mathbf{a}_b + \mathbf{w}_b$ to jointly decode $\mathbf{a}_b = (a_{N-p+1}, a_{N-p+2}, \dots, a_N)^T$ and employ the DFE procedure using $\tilde{\mathbf{R}}$ to decode $\mathbf{a}_a = (a_1, a_2, \dots, a_{N-p})^T$.

2.4.2 Parallel Detection (PD) Scheme

We can propose a new parallel detection (PD) frame work which is a compromise between the low complexity schemes and the maximum likelihood estimation (MLE). The parallel detection (PD) frame empoly the optimally ordered decision feedback equalizer (OO-DFE) act as the subdetector. We will describe the optimally OO-DFE. The received signal in complex baseband representation can be then written as

$$\mathbf{r} = \mathbf{H}\mathbf{P}^{-1}\mathbf{P}\mathbf{a} + \mathbf{w} = \tilde{\mathbf{H}}\tilde{\mathbf{a}} + \mathbf{w} \quad (2.4.2.1)$$

where \mathbf{P} is a permuted matrix representing the detection order and $\tilde{\mathbf{H}} = \mathbf{H}\mathbf{P}^{-1}$, $\tilde{\mathbf{a}} = \mathbf{P}\mathbf{a}$ represent the permuted channel matrix and the substream vector respectively. Substreams are detected recursively in the order from \tilde{a}_1 to \tilde{a}_{N_t} . The i -th detection on substream symbol \tilde{a}_i is explained in the following three steps: cancelling, nulling and ordering. For the cancelling considered : all the proceeding detected substream symbols $\hat{a}_1, \dots, \hat{a}_{i-1}$ are cancelled out from the received signal, $\mathbf{r}' = \mathbf{r} - \tilde{\mathbf{h}}_1 \tilde{a}_1 - \dots - \tilde{\mathbf{h}}_{i-1} \tilde{a}_{i-1}$ where $\tilde{\mathbf{h}}_i$ represents the i -th column of the channel matrix $\tilde{\mathbf{H}} = [\tilde{\mathbf{h}}_1, \dots, \tilde{\mathbf{h}}_{N_t}]$. For the nulling considered: a nulling vector \mathbf{g}_i^H based on zero-forcing criteria, i.e.

$$\mathbf{g}_i^H \tilde{\mathbf{h}}_{i'} = \begin{cases} 1 & i' = i \\ 0 & i' = i+1, \dots, N_t \end{cases}$$

is calculated. As a result, \mathbf{g}_i^H is the first row of $\mathbf{F}^+ = (\mathbf{F}^H \mathbf{F})^{-1} \mathbf{F}^H$ where $\mathbf{F} = [\tilde{\mathbf{h}}_i, \dots, \tilde{\mathbf{h}}_{N_t}]$. Then a hard decision on $\mathbf{g}_i^H \mathbf{r}'$ is made to obtain \hat{a}_i . For the ordering considered: we can choose the optimally ordered row from \mathbf{F}^+ as the nulling vector and make a hard decision. If

the row with smallest norm provides the largest signal-to-noise power ratio (SNR), then it can make the most reliable hard decision. We discuss the block error rate (BLER) for OO-DFE, MLE, and zero-forcing equalizer at a given channel \mathbf{H} . Firstly, we discuss the block error rate (BLER) for OO-DFE. Denote the BLER of OO-DFE algorithm by P_{oo}

$$p_{oo} \approx C \exp \frac{-d_{oo}^2}{4\sigma_w^2} \quad (2.4.2.2)$$

where $d_{oo}^2 = \min_i \frac{\Delta^2}{\mathbf{g}_i^H \mathbf{g}_i}$.

For a given \mathbf{H} , d_{oo}^2 is different if the different ordered \mathbf{P} is used. The optimal order gives the largest d_{oo}^2 . The free distance for a maximum likelihood estimation (MLE) detector where its BLER is

$$p_{MLE} \approx C \exp \frac{-d_{free}^2}{4\sigma_w^2} \quad (2.4.2.3)$$

and $d_{free}^2 = \min_{\tilde{\mathbf{a}} \neq \tilde{\mathbf{a}'}} (\tilde{\mathbf{a}} - \tilde{\mathbf{a}'})^H \mathbf{H}^H \mathbf{H} (\tilde{\mathbf{a}} - \tilde{\mathbf{a}'})$. Similarly, we can define for a zero-forcing equalizer,

$d_{ZF}^2 = \min_i \frac{\Delta^2}{[\mathbf{H}^H \mathbf{H}]_{(i,i)}^{-1}}$ where subscript (i,i) represents the diagonal element in the i -th row and

the i -th column. Intuitively, the relationship between performances of MLE, OO-DFE and zero-forcing is $P_{MLE} \leq P_{oo} \leq P_{ZF}$, which suggests $d_{free}^2 \geq d_{oo}^2 \geq d_{ZF}^2$. We will use the OO-DFE act as subdetector in parallel detector and show that.

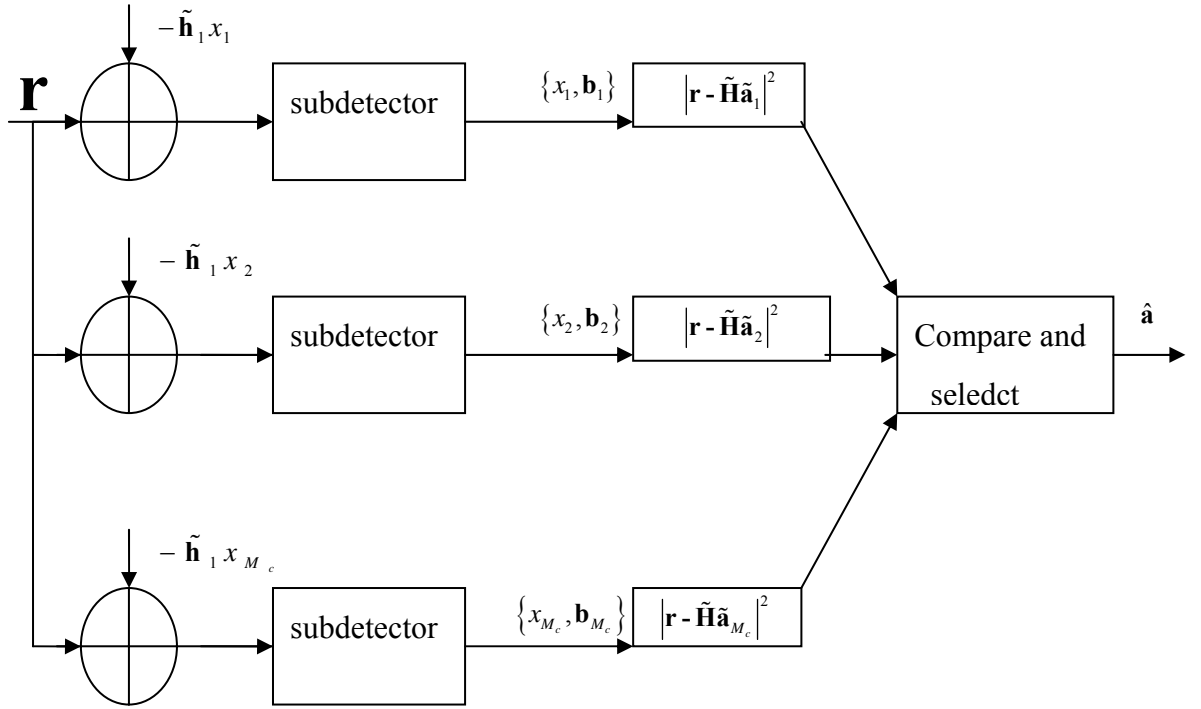


Figure 2-6 Parallel detection

We can understand when the receiver antennas $N_r > N_t$, OO-DFE can perform quite well. However, in the case $N_r = N_t$, its performance is quite far from that of the MLE. An explanation is given in this section.

The nulling vectors $\{\mathbf{g}_1, \dots, \mathbf{g}_{N_t}\}$ defined in the zero-forcing based OO-DFE algorithm are orthogonal to each other.

This can be shown easily in the following. Since the nulling vector \mathbf{g}_1^H is the first row of the pseudo-inverse matrix $[\tilde{\mathbf{h}}_1, \dots, \tilde{\mathbf{h}}_{N_t}]^+$, thus \mathbf{g}_1 must be orthogonal to $\tilde{\mathbf{h}}_2, \dots, \tilde{\mathbf{h}}_{N_t}$. Again since \mathbf{g}_i^H is the first row of $[\tilde{\mathbf{h}}_i, \dots, \tilde{\mathbf{h}}_{N_t}]^+$, \mathbf{g}_i must be a linear combination of vectors $\tilde{\mathbf{h}}_i, \dots, \tilde{\mathbf{h}}_{N_t}$. Therefore, \mathbf{g}_1 must be orthogonal to $\mathbf{g}_2, \dots, \mathbf{g}_{N_t}$. Similarly, \mathbf{g}_2 is orthogonal to $\mathbf{g}_3, \dots, \mathbf{g}_{N_t}$ as well as \mathbf{g}_1 , etc. Therefore we can conclude that the nulling vectors \mathbf{g}_i are

orthogonal to each other. The algorithm of OO-DFE is actually a process of the constructing an orthogonal set $\{\mathbf{g}_1, \dots, \mathbf{g}_{N_t}\}$ with N_t basis vectors in an N_r -dimensional space for the given channel $\tilde{\mathbf{H}}$. these vectors $\tilde{\mathbf{h}}_i, (i = 1, \dots, N_t)$ are then projected onto \mathbf{g}_i . It is not difficult to see that d_{oo} is only the shortest projection timed by Δ . Therefore, a channel $\tilde{\mathbf{H}}$ is a poor channel for OO-DFE algorithm if there exists a column whose projection is small. We show an example of $\tilde{\mathbf{H}}$ with three columns, where

$$\tilde{\mathbf{H}} = \begin{pmatrix} 2 & 1 & 0 \\ 2 & 0 & 1 \\ 0.1 & 0 & 0 \end{pmatrix}$$

Since the three $\tilde{\mathbf{h}}_i$ vectors are almost co-planar, the shortest projection is also small. In other words, since \mathbf{g}_1^H is a row of matrix $(\mathbf{F}^H \mathbf{F})^{-1} \mathbf{F}^H$, its norm certainly becomes large when matrix \mathbf{F} is near singular. We propose a new algorithm which makes the square channel matrix into a tall matrix by making hypotheses on a substream and apply the low complexity detectors on the tall channel matrix to improve the overall performance. We make hypotheses on \tilde{a}_1 and assume it is correctly subtracted from the received signal. The remaining submatrix $\tilde{\mathbf{H}}_{(2:3)} = [\tilde{\mathbf{h}}_1 \tilde{\mathbf{h}}_2]$ becomes a better channel where $d_{oo}^2(\tilde{\mathbf{H}}_{(2:3)}) = d_{free}^2(\tilde{\mathbf{H}}_{(2:3)}) = \Delta^2$.

We make all M_c hypotheses on the first substream \tilde{a}_1 and leave the remaining N_t-1 substreams to be detected by using M_c subdetectors. Therefore, the PD algorithm consists of M_c branches each with a subdetector. In the q th branch, hypothesis $\tilde{a}_1 = x_q$ is made where x_q represents the q -th point in the signal constellation. After subtracting $\tilde{\mathbf{h}}_1 x_q$ from the received signal, the q -th subdetector makes a hard decision \mathbf{b}_q on $\tilde{\mathbf{a}}_{(2:N_t)}$. For these M_c branches in the PD algorithm, each branch outputs a different hard-decision $\{x_q, \mathbf{b}_q\}$ on $\tilde{\mathbf{a}}$. Finally, a final decision $\hat{\mathbf{a}}$ is made by selecting the branch with the smallest error $|\mathbf{r} - \tilde{\mathbf{H}}_{(2:N_t)} \mathbf{b}_q - \tilde{\mathbf{h}}_1 x_q|$. Since the subdetectors are now functioning on a N_r -by- (N_t-1) matrix, the diversity is higher and they are expected to perform better. Additionally, we can further improve the performance by properly selecting the substream \tilde{a}_1 on which hypotheses are made. We analyze the BLER performance of the PD algorithm that employ OO-DFE as its subdetectors and illustrate the

method to select the optimal \tilde{a}_1 . The BLER of the PD algorithm can be written as

$$p_{PD} \approx C \exp \frac{-d_{PD}^2}{4\sigma_w^2} \quad (2.4.2.4)$$

where $d_{PD}^2 = \min(d_{free}^2, d_{oo}^2(\tilde{\mathbf{H}}_{(2:Nt)}))$. So, we find a method to choose the optimal substream on which the PD algorithm makes hypotheses. We chose \tilde{a}_1 which gives the largest $d_{oo}^2(\tilde{\mathbf{H}}_{(2:Nt)})$ that select the best submatrix of the channel to be detected by the subdetectors.

2.5 Chase Detector

We already know the large gap in both performance and complexity between the maximum-likelihood (ML) and the other existed detectors, which are linear detectors or BLAST-ordered decision-feedback (BODF) [15] detectors, hence we have the motivated search for find out a favorable performance-complexity trade-off and a unified framework which is the chase family of detection. In the chase family of detection, there is an important class of reduced-complexity detectors called list-based detectors that adopt a two-step approach of first creating a list of candidate decision vectors, and second choosing the best candidate as its final decision. For the example, the parallel detector [8] generates its list by implementing a separate low-complexity detector for each possible value of the first symbol. Numerical results suggest that if the first symbol detected is chosen so as to approximately minimize the probability of error for the remaining symbols, then the parallel detector achieves full receive diversity. This section proposes a family of Chase detectors, which includes as special cases the BODF [15], ML [5], parallel [8], PDF [16], B-CHASE [13]. Thus, the Chase family provides a unified framework for comparing a variety of existing detectors. Furthermore, we propose the B-Chase detector as a new special case that performs well on fading channels. We will demonstrate that the B-Chase detector can approach ML performance with less complexity than previously reported detectors. The B-Chase detector

distinguishes itself from previous list-based detectors in the unique way it builds its list. We will see that the B-Chase detector achieves better performance with significantly smaller candidate lists, leading to a favorable performance-complexity trade-off. We introduce the Chase detector, a general detection strategy for MIMO channels that reduces to a variety of previously reported detectors as special cases. The Chase detector defines a simple framework for not only comparing existing MIMO detection algorithms but also proposing new ones. The Chase detector is described use five steps and that is shown.

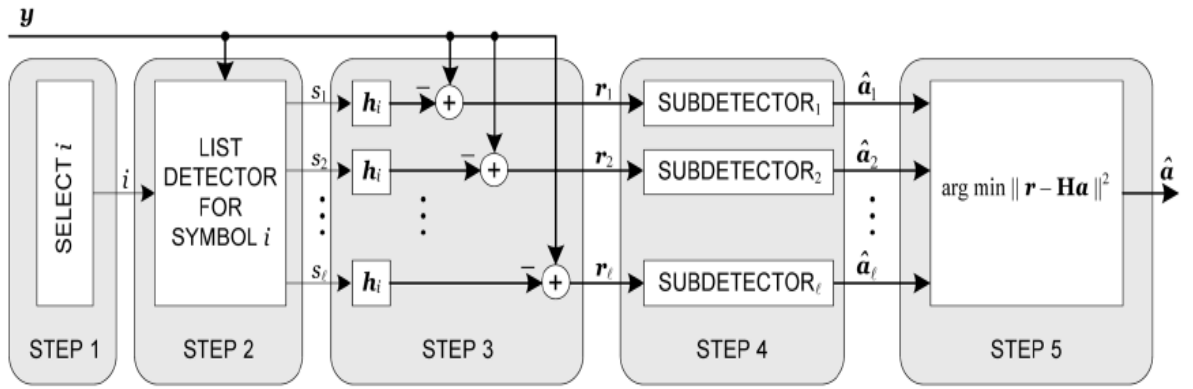


Figure 2-7 Block diagram of the Chase detector [13]

Step 1) Selecting $i \in \{1, \dots, Nt\}$ that the index of the first symbol to be detected.

Step 2) Generate a sorted list \mathcal{L} of candidate values for the i th symbol, defined as the ℓ elements of the alphabet nearest to y_i ,

$$\mathbf{y} = (\mathbf{H}^H \mathbf{H} + \alpha^2 \mathbf{I})^{-1} \mathbf{H}^H \mathbf{r} = \mathbf{F} \mathbf{r} \quad (2.5.1)$$

where \mathbf{y} is the output of either the zero-forcing (ZF) ($\alpha = 0$) or MMSE ($\alpha^2 = N_0$) linear filter.

Step 3) Generate a set of ℓ residual vectors $\{\mathbf{r}_1, \dots, \mathbf{r}_\ell\}$ by cancelling the contribution to \mathbf{r} from the i th symbol, assuming each candidate from the list is, in turn, correct:

$$\mathbf{r}_j = \mathbf{r} - \mathbf{h}_i s_j$$

Step 4) Apply each of $\{\mathbf{r}_1, \dots, \mathbf{r}_\ell\}$ to its own independent subdetector, which makes decisions about the remaining $N_t - 1$ symbols (all but the i th symbol). Together with s_j , the j th subdetector defines a candidate hard decision $\hat{\mathbf{a}}_j$ regarding the input \mathbf{a} .

Step 5) Choose as the final hard decision $\hat{\mathbf{a}}$ the candidate hard decision $\{\hat{\mathbf{a}}_1, \dots, \hat{\mathbf{a}}_\ell\}$ that best represents the observation \mathbf{r} in a minimum mean-squared-error sense:

$$\hat{\mathbf{a}} = \underset{\mathbf{a} \in \{\hat{\mathbf{a}}_1, \dots, \hat{\mathbf{a}}_\ell\}}{\arg} \min \|\mathbf{r} - \mathbf{H}\mathbf{a}\|^2 \quad (2.5.2)$$

From these steps know that have four parameters be specified:

Parameter 1: select i algorithm that affect the system performance and complexity.

Parameter 2: set the list length ℓ that affect the system performance and complexity.

Parameter 3: find the weighted filter ZF or MMSE.

Parameter 4: employ the subdetector algorithm to detect the received signal.

Table 2-3 Special cases of the Chase detector [13]

Detector	First-Symbol index i	List Length ℓ	Filter type, α	Subdetector
ML[14]	any	$ \mathbf{A} $	ZF	ML
BODF[15]	◆BLAST ₁	1	ZF or MMSE	BODF
PDF[16]	◆BLAST ₁	1	ZF or MMSE	Linear
Parallel[8]	using Selection algorithm 1	$ \mathbf{A} $	ZF	any
B-Chase[13]	using Selection	$1 \leq \ell \leq \mathbf{A} $	ZF or MMSE	BODF

	algorithm 1 or Selection algorithm 2			
--	--	--	--	--

◆The index $BLAST_1$ signifies the first index of the BLAST ordering [15]

Above that, the list length is maximal such that subdetector is likely ML detectors and the choice of which symbol to detect first is not critical to performance. The list length is one such that subdetector is likely BLAST-ordered decision-feedback (BODF) detectors and the choice of which symbol to detect first is critical to performance. The parallel detector is another Chase detector whose performance is highly sensitive to the choice of which symbol to detect first.



Chapter 3

B-Chase Detector

3.1 Introduce B-Chase Detector

We introduce the example for the B-Chase detector which is defined as a Chase detector that uses BODF as a subdetector and an SNR gain of a list detector that demonstrate the probability of error. We will see that the B-Chase detector achieves better performance with significantly smaller candidate lists, leading to a favorable performance-complexity trade-off. We can demonstrate that the B-Chase detector can approach ML performance with less complexity than previously reported detectors. We show block diagram of the B-Chase detector.

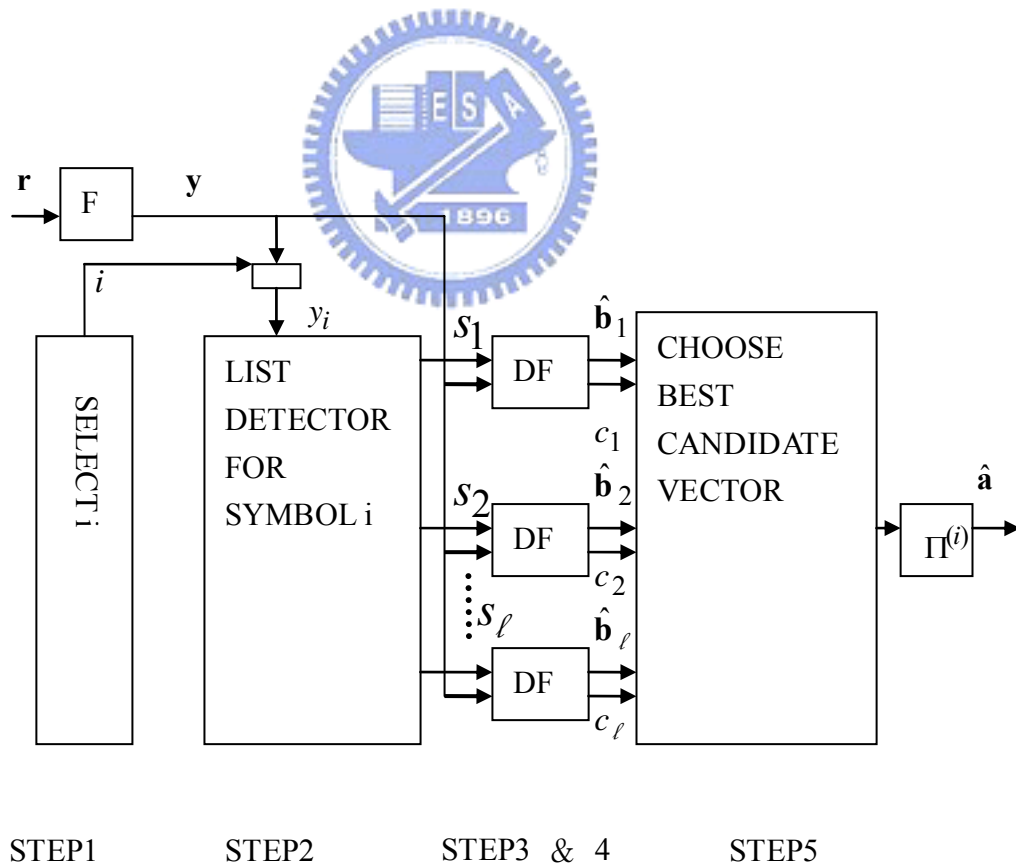


Figure 3-1 Overall block diagram for the B-Chase detector

3.1.1 The SNR Gain of a List Detector for the B-Chase Detector

We say that a list detector makes an error when the actual transmitted symbol does not appear somewhere on the list. With this definition, when we increase the length of the list that leads to a decrease in the probability of error. Therefore, we can employ the 4-QAM alphabet

to describe the list detector. For the 4-QAM alphabet $\{e^{\pm j\frac{\pi}{4}}, e^{\pm j\frac{3\pi}{4}}\}$ have a ZF front end and

the transmitted symbol is $a = e^{j\frac{\pi}{4}}$. For the i th symbol $y_i = a + n$ consider it as the input of the

list detector and $SNR_i = \frac{1}{E[|n|^2]}$. Show the correct decision regions for lists lengths $\ell \in \{1, 2, 3\}$

in the fig.3-2. Define the P_ℓ as the list-error probability and the list length is ℓ . Find that

$$P_1 = 2Q(\sqrt{SNR_i}) - Q^2(\sqrt{SNR_i}) \approx 2e^{-\frac{SNR_i}{2}} - e^{-SNR_i} \approx e^{-\frac{SNR_i}{2}} \quad (3.1.1.1)$$

$$P_2 = Q(\sqrt{2SNR_i}) \approx e^{-SNR_i} \quad (3.1.1.2)$$

$$P_3 = Q^2(\sqrt{SNR_i}) \approx e^{-SNR_i} \quad (3.1.1.3)$$

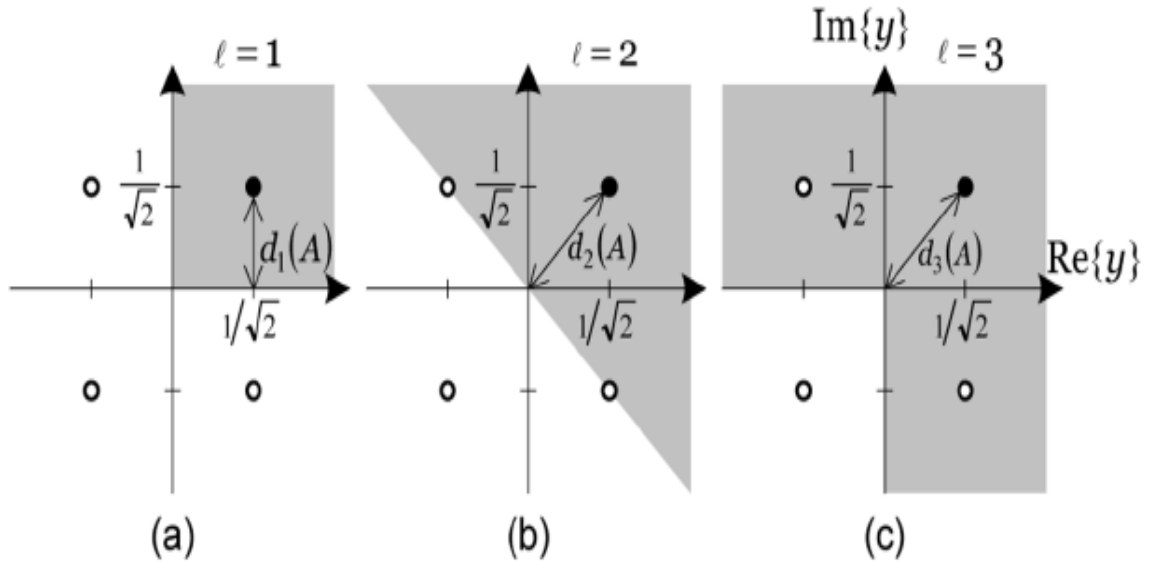
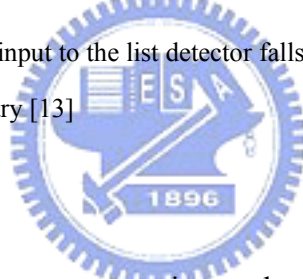


Figure 3-2 Decision regions for $a = e^{j\pi/4}$ and different list lengths: (a) $\ell = 1$; (b) $\ell = 2$; and (c) $\ell = 3$. The decision list contains a whenever the input to the list detector falls within the shaded region. Also indicated is the minimum distance d_ℓ to the boundary [13]



In the high SNR case, we can approximate the list detector SNR gain and define the $d_\ell(A)$ as the minimum distance from any element in A to the corresponding decision region boundary of the list detector with list length ℓ , so define the SNR gain γ_ℓ^2 with a list length ℓ in that

$$\gamma_\ell^2 = \frac{d_\ell^2(A)}{d_1^2(A)} \quad (3.1.1.4)$$

Show the extreme case that is the maximal list length $\ell = |A|$ and that have an infinite SNR gain $\gamma_{|A|}^2 = \infty$ because the actual transmitted symbol is on the list with $d_\ell(A) = \infty$.

3.1.2 The SNR of the B-Chase Detector

We will define the SNR for each symbol of the B-Chase detector and employ that to select which symbol is detected first. For describe that by doing the QR decomposition. Do the QR decomposition of the extended channel matrix and show that

$$\bar{\mathbf{H}} = \begin{bmatrix} \mathbf{H} \\ \alpha \mathbf{I}_{N_t} \end{bmatrix} = \tilde{\mathbf{Q}} \mathbf{L} \quad (3.1.2.1)$$

1. $\mathbf{L} = \mathbf{0}, \tilde{\mathbf{Q}} = \bar{\mathbf{H}}$
2. *for* $i = N_t, \dots, 1$
3. $l_{i,i} = |\tilde{\mathbf{q}}_i|$
4. $\tilde{\mathbf{q}}_i = \tilde{\mathbf{q}}_i / l_{i,i}$
5. *for* $j = i - 1, \dots, 1$
6. $\tilde{\mathbf{q}}_j = \tilde{\mathbf{q}}_j - l_{i,j} \cdot \tilde{\mathbf{q}}_i$
7. *end*
8. *end*

Figure 3-3 QR decomposition algorithm

Total complex of the QR decomposition algorithm is $3(N_t)^3 - 3N_r(N_t)^2 - 3(N_t)^2 - 3N_r N_t + 2N_r + 2N_t$ in the MMSE case. Where the matrix $\bar{\mathbf{H}}$ are $(N_r + N_t) \times N_t$, and where the columns of the matrix $\tilde{\mathbf{Q}}$ are orthonormal, and where \mathbf{L} is a lower triangular $N_t \times N_t$ matrix with positive and real diagonal elements. Define the bottom rows of $\tilde{\mathbf{Q}}$ are the

matrix $\alpha\mathbf{L}^{-1}$ such that $\alpha\mathbf{L}^{-1}\mathbf{L} = \alpha\mathbf{I}$. Due to (3.1.2.1) write (2.5.1) as

$$\mathbf{y} = \mathbf{U}^H \mathbf{Q}^H \mathbf{r} \quad (3.1.2.2)$$

where the matrix \mathbf{Q} is defined as the top Nr rows of $\tilde{\mathbf{Q}}$, and where $\mathbf{U}^H = \mathbf{L}^{-1}$. Use $\mathbf{r} = \mathbf{H}\mathbf{a} + \mathbf{w}$ to reduce that

$$\mathbf{y} = \mathbf{a} - \alpha^2 \mathbf{U}^H \mathbf{U} \mathbf{a} + \mathbf{U} \mathbf{Q}^H \mathbf{w} = \mathbf{a} + \mathbf{n} \quad (3.1.2.3)$$

where use $\mathbf{Q}^H \mathbf{H} = \mathbf{L} - \alpha^2 \mathbf{U}$ and define $\mathbf{n} = \mathbf{U}^H \mathbf{Q}^H \mathbf{w} - \alpha^2 \mathbf{U}^H \mathbf{U} \mathbf{a}$. Due to (3.1.2.3) that we can define the SNR and know $\tilde{\mathbf{Q}}^H \tilde{\mathbf{Q}} = \mathbf{Q}^H \mathbf{Q} + \alpha^2 \mathbf{U} \mathbf{U}^H = \mathbf{I}$ and $\alpha^2 \in \{0, N_0\}$, therefore we

can know the noise variance of the i th output of the forward filter is $E\left[|n_i|^2\right] = N_0 \|\mathbf{u}_i\|^2$, where \mathbf{u}_i is the i th column of \mathbf{U} . Define the SNR for the first symbol detected

$$SNR_1^{(i)} = \frac{\gamma_\ell^2}{N_0 \|\mathbf{u}_i\|^2} \quad (3.1.2.4)$$

and then define the next symbol detected. That is defined by the QR decomposition of the extended channel matrix $\bar{\mathbf{H}}$ whose columns are permuted, when employ the $\mathbf{\Pi}^{(i)}$ in the $\bar{\mathbf{H}}$, according to the detection order. Find the ordering and that shown.

$$\bar{\mathbf{H}} \mathbf{\Pi}^{(i)} = \tilde{\mathbf{Q}}^{(i)} \mathbf{L}^{(i)} \quad (3.1.2.5)$$

Where the columns of the $(Nr + Nt) \times Nt$ matrix $\tilde{\mathbf{Q}}^{(i)}$ are orthonormal, and where $\mathbf{L}^{(i)}$ is a lower triangular $Nt \times Nt$ matrix with positive and real diagonal elements. For the case $\tilde{\mathbf{Q}}^{(i)} = \tilde{\mathbf{Q}}$ and $\mathbf{L}^{(i)} = \mathbf{L}$ when $\mathbf{\Pi}^{(i)} = \mathbf{I}$. We can know that the $\mathbf{\Pi}^{(i)}$ is an $Nt \times Nt$ permutation

matrix that arranges the columns of $\bar{\mathbf{H}}$ such that the i th column comes first, and the remaining columns are arranged according to the BLAST ordering. Use the QR decomposition ideal to construct SNR for B-Chase detector. First, show the SNR for the first symbol detected is

$$SNR_1^{(i)} = \frac{\gamma_t^2 * (l_{1,1}^{(i)})^2}{N_0} \quad (3.1.2.6)$$

For the first symbol detected can provide list-detection gain in the B-Chase detector.

Where $l_{k,k}^{(i)}$ is the k th diagonal of $\mathbf{L}^{(i)}$ and the SNR of the final symbols can be shown.

$$SNR_k^{(i)} = \frac{(l_{k,k}^{(i)})^2}{N_0}, k = 2, \dots, Nt. \quad (3.1.2.7)$$

That $SNR_k^{(i)}, k = 2, \dots, Nt$ do not provide any list-detection gain in the B-Chase detector.



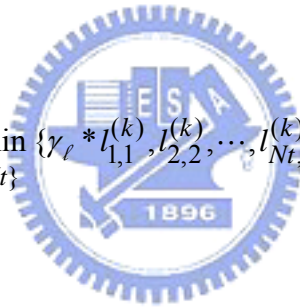
3.1.3 The B-Chase Selection

In the B-Chase detector provide the selection algorithm that get two opposing goals. Now we argue that the choice of i must balance two opposing goals: (1) the SNR of the first symbol $SNR_1^{(i)}$ is high that the list detector is likely to be correct, the actual transmitted symbol be on the list, that reduce the risk of error propagation, and (2) that the subsequent subdetectors can perform well. If our only concern is to ensure that the actual transmitted symbol can be on the list, we will choose i such that the SNR of the first symbol $SNR_1^{(i)}$ is high. For that choose i so that \mathbf{h}_i is the column of $\bar{\mathbf{H}}$ that is most orthogonal to the remaining columns which do not include \mathbf{h}_i in the remaining columns of $\bar{\mathbf{H}}$. On the other hand, if our only concern is to ensure that the subdetectors perform well when we make decisions about the remaining $Nt-1$ symbols, we will choose i so that the effective MIMO channel, we remove the \mathbf{h}_i in the column of $\bar{\mathbf{H}}$, seen by the subdetectors is as orthogonal as possible that we will get the

distance is likely the d_{free} [8]. So, we will choose i so that \mathbf{h}_i is the column of $\bar{\mathbf{H}}$ that is least orthogonal to the remaining columns in the submatrix channel, that reduce the most co-planar vectors in the submatrix channel, which is precisely the i that corresponds to the SNR of the first symbol $SNR_1^{(i)}$ is low. Therefore, to balance the two opposing goals, we should choose i so that the SNR of the first symbol $SNR_1^{(i)}$ is small, but not so small that the list does not contain the actual transmitted symbol. In other words, we should choose i so that the effective SNR of the list detector is neither too small nor too large.

That selection algorithm are shown

Selection Algorithm 1:

$$i = \arg \max_{k \in \{1, 2, \dots, Nt\}} \min \{ \gamma_\ell * l_{1,1}^{(k)}, l_{2,2}^{(k)}, \dots, l_{Nt, Nt}^{(k)} \} \quad (3.1.3.1)$$


That maximizes the minimum SNR of the symbols. To implement the selection algorithm 1 can spend the complexity is $O(Nt^4)$ computations when $\ell > 1$. From the QR decomposition their complexity is $O(Nt^3)$ computations, therefore the selection algorithm 1 implement Nt times. Due to the selection algorithm 1 complexity is high, so find the low-complexity to implement the selection algorithm. That will be shown the selection algorithm 2 which can reduce the complexity but can has the bad performance. Since the smallest SNR inside the subdetector is $SNR_2^{(i)}$ when $1 < \ell < |A|$, select the symbol which maximizes the minimum of $SNR_1^{(i)}$ and $SNR_2^{(i)}$. $SNR_2^{(i)}$ is shown.

$$SNR_2^{(i)} = \frac{1}{N_0 \min_{j \neq i} \{ \|\mathbf{u}_j\|^2 - |g_{j,i}|^2 \}} \quad (3.1.3.2)$$

where $g_{j,i} = \frac{\mathbf{u}_j^H \mathbf{u}_i}{\|\mathbf{u}_i\|}$

Selection algorithm 2 is shown:

$$i = \begin{cases} \arg \max_{k \in \{1, 2, \dots, Nt\}} \|\mathbf{u}_k\|^2 & \ell = |A| \\ \arg \max_{k \in \{1, 2, \dots, Nt\}} \min \left\{ \frac{\gamma_\ell^2}{\|\mathbf{u}_k\|^2}, \frac{1}{\min_{j \neq i} \{ \|\mathbf{u}_j\|^2 - |g_{j,i}|^2 \}} \right\} & , else. \end{cases} \quad (3.1.3.3)$$

The $Nt(Nt-1)$ squared-magnitudes $\left\{ |g_{j,i}|^2 \mid 1 < j < Nt, 1 < i < Nt, j \neq i \right\}$ are computed in selection algorithm 2. The each squared-magnitude is need to compute the complexity is $5Nt$.

Table 3-1 Complexity of the selection algorithm 1 and the selection algorithm 2

	total complex	Nr=Nt=N=4
The selection algorithm 1	$3.5*Nr*(Nt)^3+3.5(Nt)^4+0.5Nr*(Nt)^2+0.5(Nt)^3$	1856
The selection algorithm 2	$3.5*Nr*(Nt)^2+3.5(Nt)^3+0.5Nr*Nt+0.5(Nt)^2+5(Nt)^3-5(Nt)^2$	704



3.1.4 Implementing the B-Chase Detector

We will implement the B-Chase detector and show the block diagram in the fig.3-1, and the pseudocode in the fig.3-4, and fig.3-5. For the B-Chase detector use the selection algorithm 1 or the selection algorithm 2. Now it use the selection algorithm 1 to implement in the B-Chase detector. For the selection algorithm 1 we must compute the QR decomposition to get $\mathbf{L}^{(i)}$ such that use the selection algorithm 1 to decide which symbol to detect but we do not compute directly that. We use another method to compute the QR decomposition to get $\mathbf{L}^{(i)}$.

From the $\mathbf{\Pi}^{(i)}$ definition we know permute the columns of $\bar{\mathbf{H}}$ by $\mathbf{\Pi}^{(i)}$ that is similar to permute the the rows of $\mathbf{C} = \mathbf{U}^H \tilde{\mathbf{Q}}^H$ by $\mathbf{\Pi}^{(i)H}$. So we define the sorted-QR decomposition of \mathbf{C}^H and that is shown.

$$\mathbf{C}^H \mathbf{\Pi}^{(i)} = \tilde{\mathbf{Q}}^{(i)} \mathbf{U}^{(i)} \quad (3.1.4.1)$$

We can use the relation $\mathbf{U}^{(i)} = (\mathbf{L}^{(i)H})^{-1}$ to get $\mathbf{L}^{(i)}$. From the $\mathbf{\Pi}^{(i)}$ definition is the i th column of \mathbf{C}^H comes first, so modify the sorted-QR decomposition. We can use the algorithm of the sorted-QR decomposition to compute the sorted-QR decomposition after modify this such that the i th column of \mathbf{C}^H firstly comes. Form the (3.1.4.1) equation we can modify that

$$\mathbf{C}^H \mathbf{\Pi}^{(i)} = \tilde{\mathbf{Q}} \mathbf{U} \mathbf{\Pi}^{(i)} = \tilde{\mathbf{Q}} \mathbf{\Theta}^{(i)} \mathbf{\Theta}^{(i)H} \mathbf{U} \mathbf{\Pi}^{(i)} \quad (3.1.4.2)$$

where $\mathbf{\Theta}^{(i)}$ is a unitary matrix such that the $\mathbf{U}^{(i)} = \mathbf{\Theta}^{(i)H} \mathbf{U} \mathbf{\Pi}^{(i)}$ is an upper triangular matrix with real and positive diagonals and form (3.1.4.2) and (3.1.4.1) equations we can define the relation $\tilde{\mathbf{Q}}^{(i)} = \tilde{\mathbf{Q}} \mathbf{\Theta}^{(i)}$. We can define the \mathbf{U} sorted-QR decomposition and show

$$\mathbf{U} \mathbf{\Pi}^{(i)} = \mathbf{\Theta}^{(i)} \mathbf{U}^{(i)} \quad (3.1.4.3)$$

Form the $\mathbf{y} = (\mathbf{H}^H \mathbf{H} + \alpha^2 \mathbf{I})^{-1} \mathbf{H}^H \mathbf{r} = \mathbf{F} \mathbf{r}$ equation we can define the front-end filter \mathbf{F} as that

$$\mathbf{F} = \mathbf{D}^{-1} \mathbf{Q}^{(i)H} = \mathbf{D}^{-1} \mathbf{\Theta}^{(i)H} \mathbf{Q}^H \quad (3.1.4.4)$$

where \mathbf{D} is a diagonal matrix with $d_{j,j} = l_{j,j}^{(i)}$. Form the $\mathbf{y} = \mathbf{F} \mathbf{r}$ and $\mathbf{r} = \mathbf{H} \mathbf{a} + \mathbf{w}$ equations we can reduce that as

$$\mathbf{y} = \mathbf{M} \mathbf{b} + \mathbf{n} \quad (3.1.4.5)$$

where $\mathbf{M} = \mathbf{D}^{-1} \mathbf{L}^{(i)}$ is an $N_t \times N_t$ lower-triangular matrix with ones along the diagonal, where $\mathbf{b} = \mathbf{\Pi}^{(i)H} \mathbf{a}$ is a permuted version of the channel input, and the effective noise is $\mathbf{n} = \mathbf{F} \mathbf{w} - \alpha^2 \mathbf{D}^{-1} \mathbf{U}^{(i)} \mathbf{b}$. From the B-Chase preprocessing function we can get some parameters $\mathbf{F}, \mathbf{M}, \mathbf{\Pi}^{(i)}$, and $\{d_{1,1}^2, \dots, d_{N_t, N_t}^2\}$. Use these parameters in the B-Chase detector to implement that. We employ the list detector to generate an ordered list $[s_1, \dots, s_\ell]$ of the ℓ elements of \mathbf{A}

that are nearest to y_1 which is 1th element of \mathbf{y} . For the ordered list $[s_1, \dots, s_\ell]$, s_i is in the ordered list and it is the i th closest element of \mathbf{A} that is nearest to y_1 . From the list detector generate an ℓ elements ordered list and then use \mathbf{y} and the ordered list as inputs of the ℓ DF detectors whose first symbol decisions are hard-wired to decide first outputs of DF detectors and then compute the first cost. The next steps use a decision-feedback process to decide other symbols and update the cost. For show that the l th subdetector cancels the intersymbol interference from the k th element of as follows:

$$x_{k,l} = y_k - \sum_{j=1}^{k-1} m_{k,j} \hat{b}_{j,l} \quad (3.1.4.6)$$

Where $\hat{b}_{j,l} = \text{dec}\{x_{j,l}\}$ is the decision that regard that as the j th element of $\hat{\mathbf{b}}_l$ which is the decision vector of the l th subdetector, and where $\text{dec}\{x\}$ quantizes x to the nearest element of \mathbf{A} . From the outputs of subdetectors, B-Chase detector choose the minimum cost of the outputs of subdetectors as the decision vector. To express the cost of the l th decision vector as $c_l = \|\mathbf{r} - \mathbf{H}\Pi^{(i)}\hat{\mathbf{b}}_l\|^2$, which reduces to

$$c_l = \|\mathbf{D}(\mathbf{y} - \mathbf{M}\hat{\mathbf{b}}_l)\|^2 \quad (3.1.4.7)$$

FUNCTION BCHASE DETECTOR

INPUTS : $\bar{\mathbf{H}}, \ell, \mathbf{A}$

OUTPUT : $\hat{\mathbf{a}}$

=====

1. $\{\mathbf{F}, \mathbf{M}, \mathbf{\Pi}^{(i)}, \{d_{j,j}^2\}\} = BChasePreprocessing(\bar{\mathbf{H}}, \ell)$
2. $\mathbf{y} = \mathbf{F}\mathbf{r}$
3. $[s_1, \dots, s_\ell] = ListDetect(y_1 | \mathbf{A}, \ell)$,
so that s_i is the i -th closest element of \mathbf{A} to y_1
4. $\tau = \infty$
5. for $l = 1$ to ℓ ,
6. $\hat{b}_l = s_l$
7. $c_l = d_{1,1}^2 |y_1 - s_l|^2$
8. for $k = 2$ to Nt ,
9. if $c_l < \tau$,
10. $x = y_k - \sum_{j=1}^{k-1} m_{k,j} \hat{b}_{j,l}$
11. $\hat{b}_{k,l} = dec\{x\}$
12. $c_l = c_l + d_{k,k}^2 |x - \hat{b}_{k,l}|^2$
13. end
14. end
15. if $c_l < \tau$,
16. $\tau = c_l$
17. $f = l$
18. end
19. end
20. $\hat{\mathbf{a}} = \mathbf{\Pi}^{(i)} \mathbf{b}_f$

Figure 3-4 Computationally efficient implementation of the B-Chase detector [13]

FUNCTION BCHASEP REPROCESSING

INPUTS : $\bar{\mathbf{H}}, \ell$

OUTPUTS : $\mathbf{F}, \mathbf{M}, \mathbf{\Pi}^{(i)}, \{d_{1,1}^2, \dots, d_{N_t, N_t}^2\}$

1. $[\tilde{\mathbf{Q}}, \mathbf{L}] = QRdecomposition(\bar{\mathbf{H}})$
2. $\mathbf{U} = (\mathbf{L}^H)^{-1}$
3. for $j = 1$ to N_t , $e_j = \sum_{k \in \{1, \dots, j\}} |u_{k,j}|^2$, end
4. for $k = 1$ to N_t ,
5. $[\Theta^{(k)}, \mathbf{U}^{(k)}, \mathbf{\Pi}^{(i)}, \{(l_{1,1}^{(k)})^2, \dots, (l_{N_t, N_t}^{(k)})^2\}] = sortedQR(\mathbf{U}, \mathbf{e}, k)$
6. $S^{(k)} = \min \{(\Upsilon_\ell * l_{1,1}^{(k)})^2, (l_{2,2}^{(k)})^2, \dots, (l_{N_t, N_t}^{(k)})^2\}$
7. end
8. $i = \arg \max_{k \in \{1, \dots, N_t\}} S^{(k)}$
9. $\mathbf{D}^{-1} = diag(\mathbf{U}^{(i)})$
10. $\mathbf{Q} =$ first N_r rows of $\tilde{\mathbf{Q}}$
11. $\mathbf{F} = \mathbf{D}^{-1} \Theta^{(i)H} \mathbf{Q}^H$
12. $\mathbf{M} = \mathbf{D}^{-1} \Theta^{(i)H} \mathbf{L} \mathbf{\Pi}^{(i)}$
13. for $j = 1$ to N_t , $d_{j,j}^2 = (l_{j,j}^{(k)})^2$ end

Figure 3-5 Preprocessing pseudocode for the proposed implementation of the B-Chase detector that uses selection algorithm 1 [13]

We can have two crucial things that reduce the complexity.

- From compute the sorted-QR decomposition algorithm of \mathbf{U} and the QR decomposition algorithm of $\bar{\mathbf{H}}$ that we know the $m_{k,k} = 1$ element of the \mathbf{M} matrix.

And then we can combine the equation (3.1.4.6) and the equation (3.1.4.7) that let

we can rewrite the cost expression as

$$c_l = \sum_{k=1}^{N_t} d_{k,k}^2 |x_{k,l} - \hat{b}_{k,l}|^2 \quad (3.1.4.8)$$

From that we reduce computations in the cost equation (3.1.4.8) in the subdetector.

We can use the $O(Nt)$ computations.

- We can use a pruning and threshold-tightening strategy that can reduce the computations. A cost threshold can be established with the cost c_1 of the first subdetector's decision. In subsequent subdetectors, we can abort both the cost calculation (3.1.4.8) as well as the decision feedback process (3.1.4.7) whenever this threshold is exceeded the cost threshold. Furthermore, the threshold can be reduced each time a lower cost is found.

We will get the performance and complexity well. From the B-Chase detector know the channel parameters that Rayleigh-fading gain, and know N_0 . We can use B-Chase*(ℓ) to denote the B-Chase detector with list length ℓ , $\alpha^2 = N_0$, and use selection algorithm (3.1.3.1). We can use B-Chase(ℓ) to denote the B-Chase detector with list length ℓ , $\alpha^2 = N_0$, and use selection algorithm (3.1.3.3). We use input is 4 with 16-QAM and output is 4. And show figure the performance versus the number of antennas, where the SNR per bit is

$$\frac{E[\|\mathbf{H}\mathbf{a}\|^2]}{(E[\|\mathbf{w}\|^2]) * \log_2 |A|} = \frac{E[\mathbf{a}^H \mathbf{H}^H \mathbf{H} \mathbf{a}]}{(E[\|\mathbf{w}\|^2]) * \log_2 |A|}.$$

Where $E[\mathbf{H}^H \mathbf{H}] = Nr\mathbf{I}_{N_t}$, $E[\mathbf{w}^H \mathbf{w}] = NrN_0$, and $E[\mathbf{a}^H \mathbf{a}] = NtE[a^H a]$. We can reduce that as

$$SNR = \frac{NtE[a^H a]}{N_0 \log_2 |A|}$$

For define the unit that is real multiplies (RMs) per bit to describe the complexity. We define the squared absolute value of a complex number is counted as two RM, and the complex multiplications are counted as three RMs. Now we define the preprocessing complexity that need to compute the computations that are required only once per channel estimation. And define the core-processing complexity need to compute the computations that must be implemented during every symbol period. In the B-Chase detector show the core-processing complexity when $\ell = 1$ show their core-processing complexity is $3NrNt$ RM and when $\ell \neq 1$ show their core-processing complexity is $3(Nr+\ell)Nt$ RM. The overall complexity includes both core-processing complexity and preprocessing complexity. We assume that the channel estimate is updated in T symbol periods. That unit is real multiples per bit. We can show that as:

$$complexity = \frac{C_{core} + C_{pre} / T}{Nt \log_2 |A|} \quad (3.1.4.9)$$

From preprocessing complexity we can know the state of the channel to compute complexity in the B-Chase detector. If the state of the channel changes quickly, then we can estimate the state of the channel is quick in the small symbol periods. That can affect the preprocessing complexity. If we have the small preprocessing complexity, then that reduce the complexity in the state of the channel changes quickly.

Table 3-2 System parameters

Transmit antenna	4
Receive antenna	4
Channel is updated in T symbol periods	8
Rayleigh-fading	Mean=0, Varance=1
Channel order	0
Selection algorithm	1
List length ℓ	1, 2, and 16

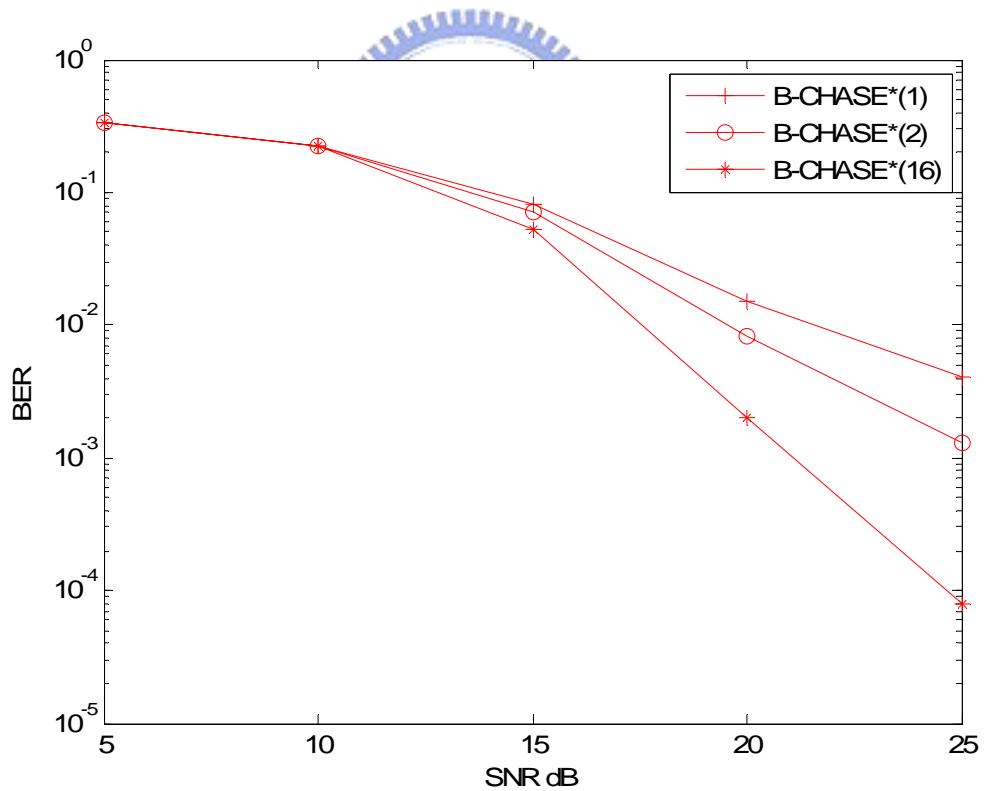


Figure 3-6 The bit error rate versus SNR for the B-Chase detector* (ℓ) with $\ell=1, 2, 16$, T=8, and 16 QAM

From figure we can know when increase the length of the list that leads to a decrease in the probability of error. In other word shrink this gap and provide new solutions for managing the inherent performance-complexity trade-off in MIMO detection. We can find that shrink this gap quickly in the low the length of the list.

Table 3-3 System parameters

Transmit antenna	4
Receive antenna	4
Channel is updated in T symbol periods	8
Rayleigh-fading	Mean=0, Varance=1
Channel order	0
Selection algorithm	1 and 2
List length ℓ	1 ,and 2

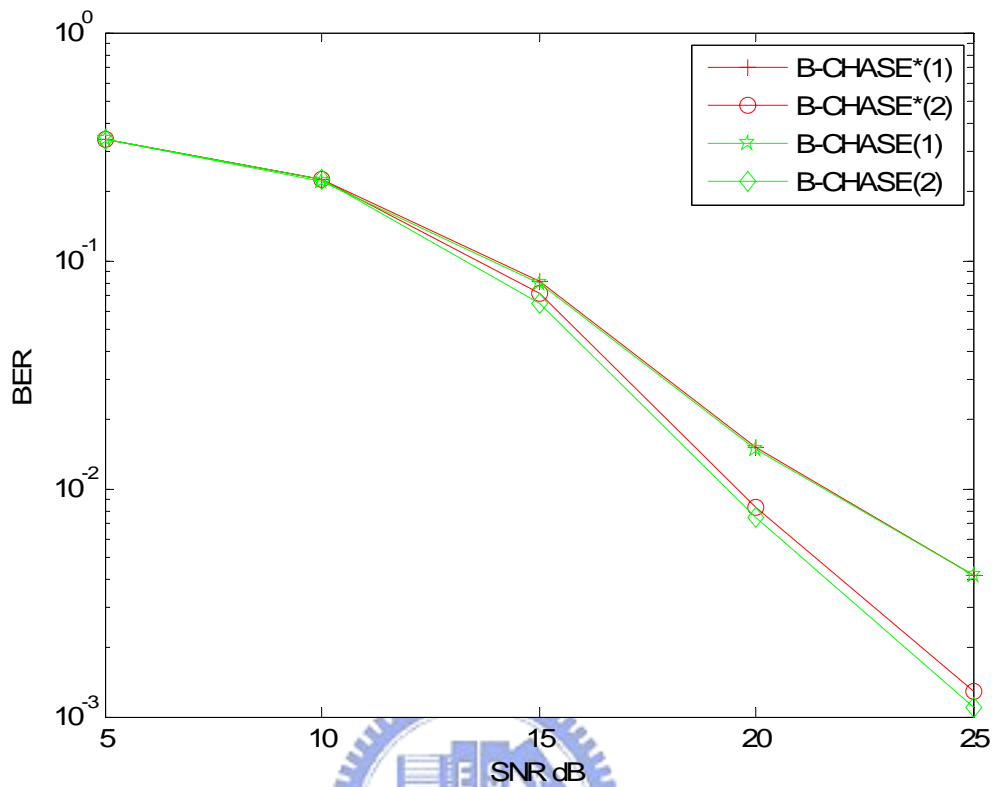


Figure 3-7 Bit error rate versus SNR for the B-Chase detector* (ℓ) and the B-Chase detector (ℓ) with $\ell=1,2$, $T=8$, and 16 QAM

From figure we can know selection algorithm 1 and selection algorithm 2 that have almost the same performance.

Table 3-4 System parameters

Transmit antenna	4
Receive antenna	4
Channel is updated in T symbol periods	8
Rayleigh-fading	Mean=0,Varance=1
Channel order	0
Selection algorithm	1
List length ℓ	1 ,and 2

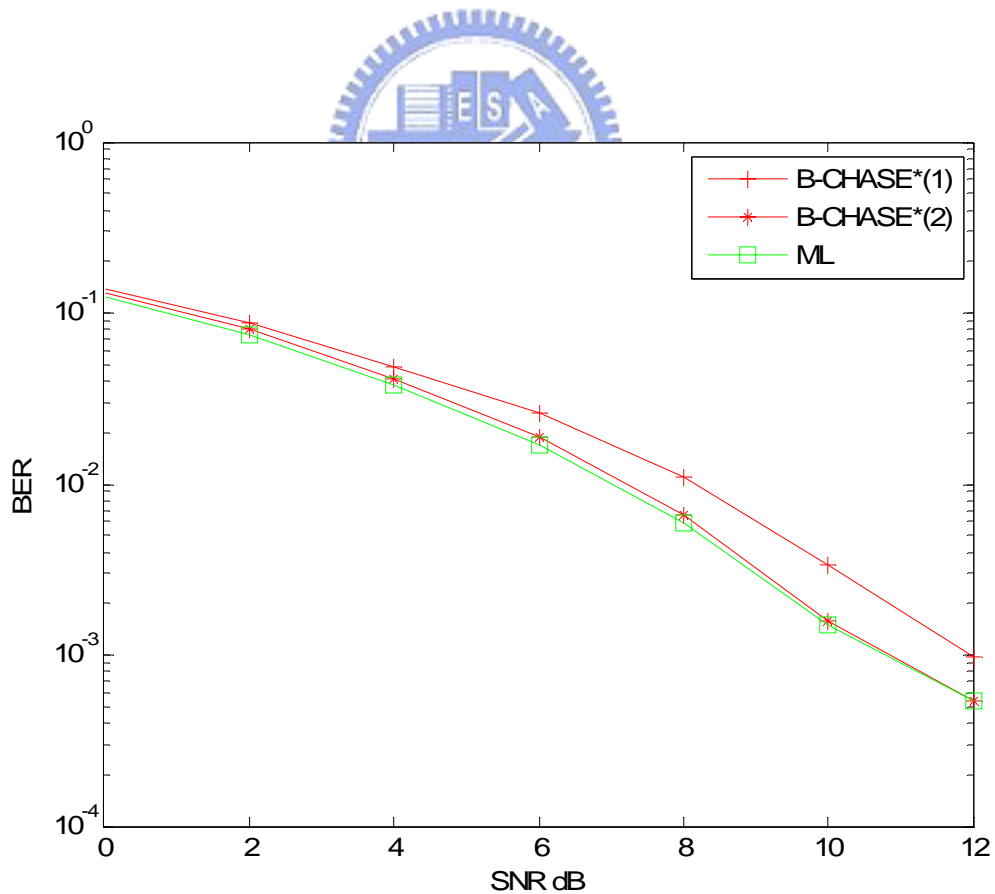


Figure 3-8 Bit error rate versus SNR for the B-Chase detector* (ℓ) with $\ell=1,2$, and the ML detector T=8, and BPSK

From figure we can know the B-Chase detector is nearly ML detector.

Table 3-5 Complexity for B-Chase Detector and ML Detector

	Function B-Chase Preprocessing complexity	Function B-Chase detector complexity	Channel is updated in T symbol periods	Total complexity	Nr=Nt=4 , QPSK(A=4) ,T=8 , $\ell=4$
B-Chase *(ℓ) detector	$3.5(Nt)^4 + 3.5Nr(Nt)^3 + 6.5(Nt)^3 - 2.5Nr(Nt)^2 + 0.5(Nt)^2 + 2Nr + 11Nt$	$3NtNr + 3Nt + 2\ell + 2.5\ell(Nt)^2 - 0.5\ell Nt$		$[3.5(Nt)^4 + 3.5Nr(Nt)^3 + 6.5(Nt)^3 - 2.5Nr(Nt)^2 + 0.5(Nt)^2 + 2Nr + 11Nt] + T$ $[3NtNr + 3Nt + 2\ell + 2.5\ell(Nt)^2 - 0.5\ell Nt]$	3868
ML detector				$[3NrNt + 2Nr] A^{Nt}$	114688

3.1.5 The B-Chase Detector for Channel Estimation Errors

In previous sections, we always assumed that we have perfect the channel state information (CSI) at the receiver, which allows us to compare the performance. However, the channel information is typically not perfect. A channel estimator extracts from the received signal approximate channel coefficients during the transmission symbol. One method to accomplish this is to transmit the training signal prior to the transmission symbol. That are used as preamble at the start of each frame. Another way to estimate the channel fading coefficients is to embed the pilot bits, that is called pilot signal, inside the signal.

The impact from the channel estimation errors will degrade the performance of the system. To study the impact of the channel estimation errors on the B-CHASE detector algorithm, we introduce the error model at the receiver.

$$\mathbf{H}' = \mathbf{H} + \Delta\mathbf{H} \quad (3.1.5.1)$$

where \mathbf{H} represent the true channel matrix and $\Delta\mathbf{H}$ denotes the channel estimation error. The elements of $\Delta\mathbf{H}$ are assumed to be zero mean, variance is 0.01 and complex Gaussian. The B-CHASE*(16) is a measurement based on that we can accurately obtain the channel estimation. The B-CHASEer*(16) is a measurement based on that we can not accurately obtain the channel estimation. As shown in Figure, the channel estimation errors with The B-CHASEer*(16) given the B-CHASE decoding algorithm. It is clear from the figure, the B-CHASEer*(16) decoding algorithm starts to perform poorly. This poor performance is caused by inter-symbol interference (ISI).When we obtain the error channel matrix, find out the error outputs, $\mathbf{F}' \mathbf{M}'$ etc., in the B-Chase preprocessing. From that obtain the error $\mathbf{y}' = \mathbf{F}' \mathbf{r}$ produce the ISI. This cause a ISI problem since channel estimation error is the biggest contributor of the errors in the simulation at the high SNR region.

Table 3-6 System parameters

Modulation	16-QAM
Transmit antenna	4
Receive antenna	4
Channel is updated in T symbol periods	8
Rayleigh-fading	Mean=0, Varance=1
Error of the Rayleigh-fading	Mean=0, Varance=0.01
Channel order	0
Selection algorithm	1
List length ℓ	16

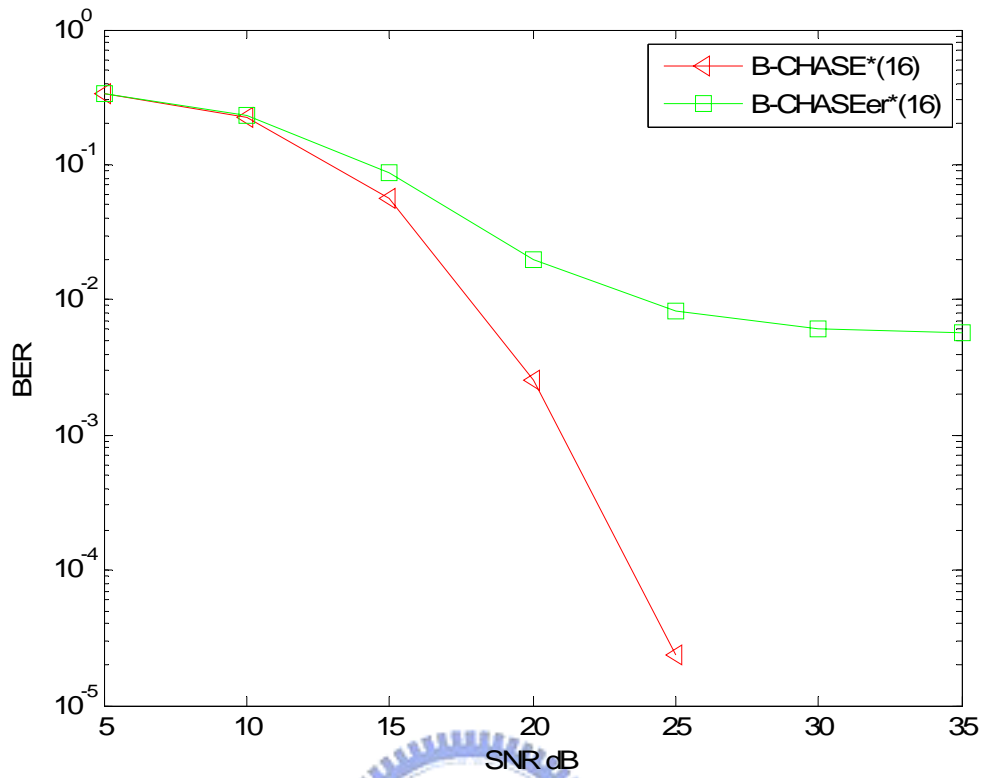


Figure 3-9 Bit error rate with channel estimation error and without channel estimation error



From figure we can know the channel estimation error demonstrate the error in the high SNR.

Chapter 4

B-Chase Detector of MIMO-OFDM Systems

The material in this Chapter is largely taken from [9], [10], [11], and [12].

4.1 OFDM System Models

We understand the single carrier (SC) that has the poor spectral efficiency in our communication system and when we have multipath so that have frequency selective fading and inter-symbol interference (ISI). So, we will employ the principle of multi carrier(MC) system that can combat them because only some subcarriers is fail to communication. We use orthogonal frequency division multiplexing (OFDM) that is to divide the available spectrum into several subchannels (subcarriers) and the frequency response of the subchannels are overlapping and orthogonal. That get the channel is flat fading per subcarrier and decrease ISI. In the MC system the transmitter separate the data stream into several parallel ones and each modulated by a specific subcarrier that can use Inverse discrete Fourier Transform (IDFT) to implemt that in the baseband modulation. In the receive each demodulated by a specific subcarrier that can use discrete Fourier Transform (DFT) to implement that in the baseband demodulation.

When OFDM symbols pass through a time-dispersive channel, inter-symbol interference (ISI) and inter-carrier interference (ICI) usually occur in the receiver and cyclic prefix (CP) is introduced to combat ISI and ICI. Cyclic prefix, shown in Figure 4.1, is a copy of the tail part of a OFDM symbol is attached to its front. As long as the cyclic prefix length is longer than its experiencing time-dispersive channel length, ISI can be avoided. At the same time, the cyclic prefix along with its OFDM symbol makes a periodic OFDM signal and maintains the properties of circular convolution and subcarrier orthogonality that prevents the ICI effect.

For this system we employ the following assumptions:

- The channel impulse response is shorter than the cyclic prefix.
- Transmitter and receiver are perfectly synchronized.
- The fading is slow enough for the channel to be considered constant during one OFDM symbol interval.
- Channel noise is additive, white, and complex Gaussian.

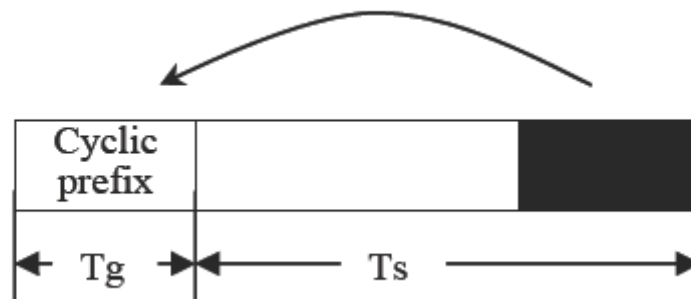


Figure 4-1 Cyclic prefix of an OFDM symbol [10]

4.1.1 Continuous-Time Model

In this chapter, a continuous-time model is used to introduce the whole OFDM baseband system including the transmitter and receiver. In the transmitter, the transmitted data is split into multiple subchannels with overlapping frequency bands. The spectrum of OFDM signal is shown in Figure 3.2. It is clear that the spectrum of each subchannel is spreading to all the others, but is zero at all the other subcarrier frequencies, because of the sinc function property, which is the key feature of the orthogonality.

Assumeing an OFDM system with N subcarriers, a bandwidth of W Hz and a symbol length of T seconds, of which T_g seconds is the length of the cyclic prefix, the transmitter uses the following waveforms

$$\Phi_k(t) = \begin{cases} \frac{1}{\sqrt{T-T_g}} e^{j2\pi\frac{W}{N}k(t-T_g)} & \text{if } t \in [0, T] \\ 0, & \text{otherwise} \end{cases} \quad (4.1.1.1)$$

Where $T = N/W + T_g$. Note that $\Phi_k(t) = \Phi_k(t + N/W)$ when t is within the cyclic prefix $[0, T_g]$. Since $\Phi_k(t)$ is a rectangular pulse modulated on the carrier frequency kW/N , the common interpretation of OFDM is that it uses N subcarriers, each carrying a low bit-rate. The waveforms $\Phi_k(t)$ are used in the modulation and the transmitted baseband signal for OFDM symbol as

$$x(t) = \sum_{k=0}^{N-1} X(k)\Phi_k(t) \quad (4.1.1.2)$$


Where $X(1), X(2), \dots, X(N-1)$ are complex numbers from a set of signal constellation points. Assume the given channel is quasi-static, i.e., constant during the transmission of an OFDM symbol, where the quasi-static impulse response is $h(\tau; t)$ of the physical channel is restricted to the interval $\tau \in [0, T_g]$, i.e., to the length of the cyclic prefix. The received signal becomes

$$y(t) = (h \times x)(t) = \int_0^{T_g} h(\tau; t)x(t-\tau)d\tau + n(t) \quad (4.1.1.3)$$

where n is additive, white, and complex Gaussian channel noise.

The OFDM receiver consists of a filter bank, matched to the last part $[T_g, T]$ of the transmitter waveforms $\Phi_k(t)$, i.e.,

$$\psi_k(t) = \begin{cases} \Phi_k^*(T-t) & \text{if } t \in [0, T-T_g] \\ 0, & \text{otherwise.} \end{cases} \quad (4.1.1.4)$$

Calculating the sampled output at the k th matched filter.

$$\begin{aligned} Y(k) &= (y \times \psi_k)(t) \Big|_{t=T} \\ &= \int_{-\infty}^{\infty} y(t) \psi_k(T-t) dt \\ &= \int_{T_g}^T \left(\int_0^{T_g} h(\tau; t) \left[\sum_{k'=0}^{N-1} X(k') \Phi_{k'}(t-\tau) \right] d\tau \right) \Phi_k^*(t) dt \\ &\quad + \int_{T_g}^T n(T-t) \Phi_k^*(t) dt \end{aligned} \quad (4.1.1.5)$$

Figure 4.3 shows a typical continuous-time OFDM baseband modulator, in which the transmitted data is split into multiple parallel streams which are modulated by different subcarriers and then transmitted simultaneously. At the receiver, the received signal is demodulated simultaneously by multiple matched filters and then the data on each subchannel is obtained by sampling the outputs of matched filters, as shown in Figure 4.4.

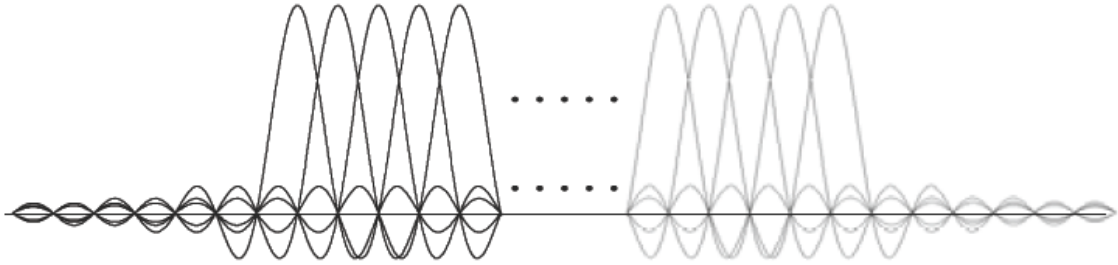


Figure 4-2 Spectrum of an OFDM signal [10]

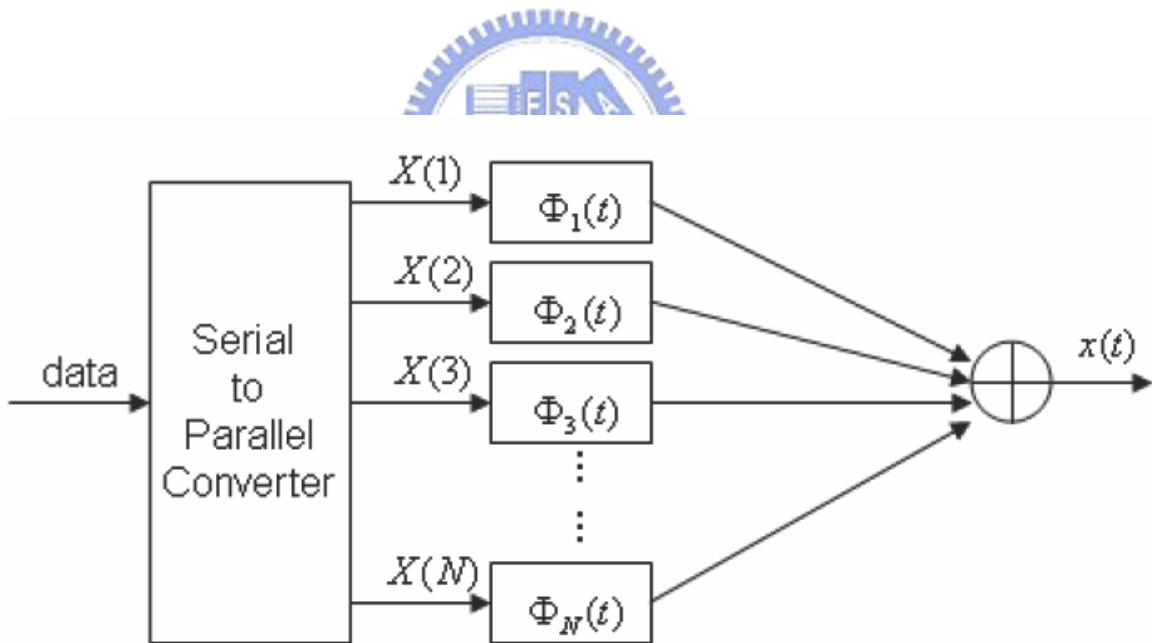


Figure 4-3 Continuous-time OFDM baseband modulator [10]

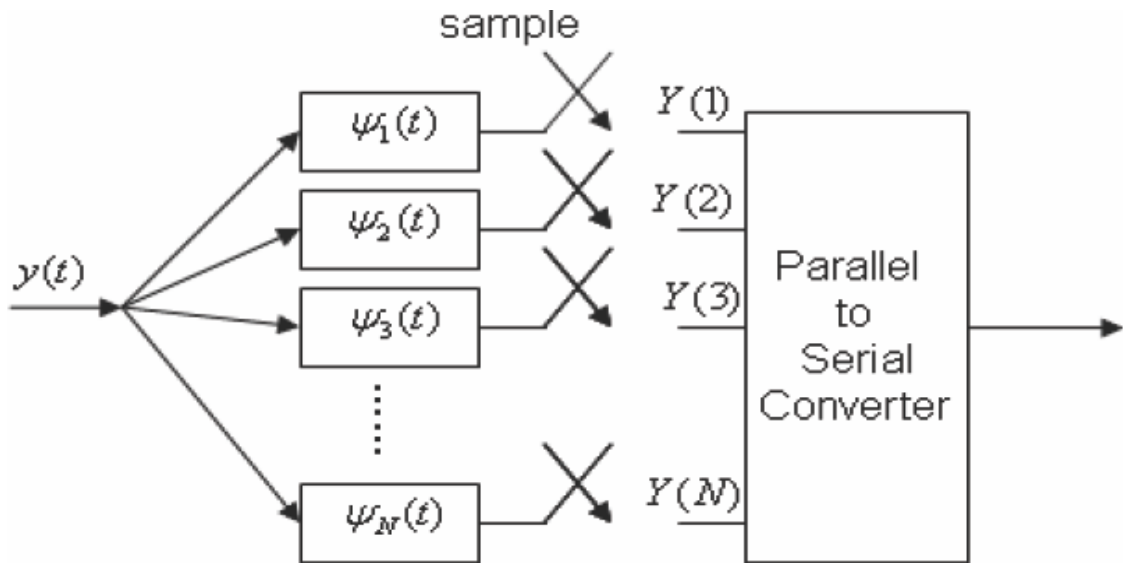


Figure 4-4 Continuous-time OFDM baseband demodulator [10]



4.1.2 Discrete-Time Model

To simultaneously transmit multiple data, the transmitter must modulate data with multiple subcarriers and the receiver must demodulate with multiple matched filters. In fact, the modulation and demodulation can be implemented efficiently by using digital IDFT/DFT operations, because they can be respectively represented as

$$x(i) = \sum_{k=0}^{N-1} X(k)e^{j\frac{2\pi}{N}ki} = \sum_{k=0}^{N-1} X(k)\Phi_k(i) \quad (4.1.2.1)$$

$$Y(k) = \sum_{i=0}^{N-1} y(i)e^{-j\frac{2\pi}{N}ki} = \sum_{i=0}^{N-1} y(i)\Psi_k(i) \quad (4.1.2.2)$$

which are the same as IDFT operation of the transmitted data $X(k)$ and DFT operation of the received data $y(i)$, respectively.

Figure 4-5 shows the discrete-time baseband OFDM model. The IDFT transforms the frequency-domain data into time-domain data which is delivered over the air and passed through a multi-path channel, denoted as $h(n,m)$ n is the time index and m is the channel path delay. At the receiver, to recover the signal in frequency domain, DFT is adopted in the demodulator as a matched filter. Then the frequency-domain signal of each subchannel is obtained from its DFT output.

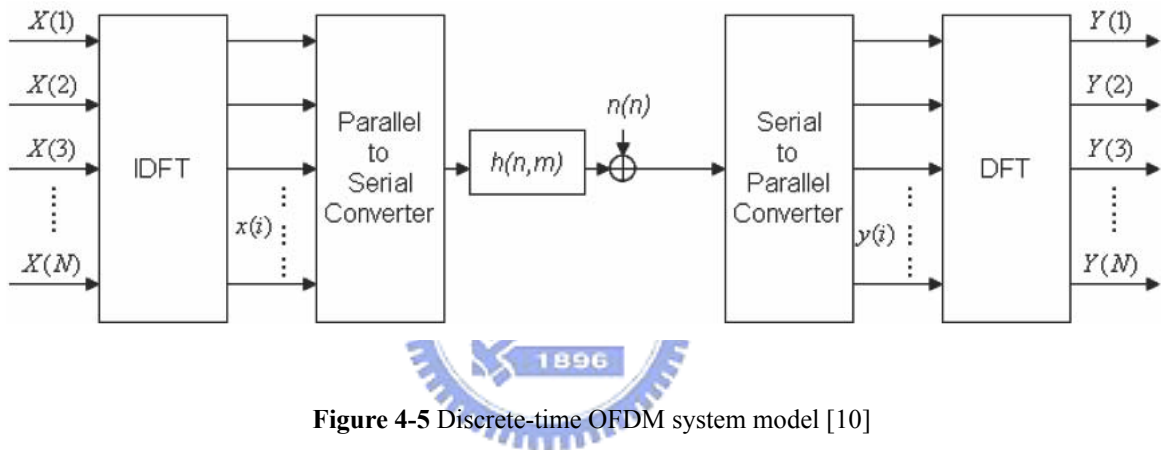


Figure 4-5 Discrete-time OFDM system model [10]

4.1.3 Effect of Cyclic Prefix

Because of multipath channels, orthogonality as shown in Figure 4.2 will be destroyed by ISI and ICI. However, as long as the cyclic prefix length is longer than the channel order of $h(n,m)$, ISI effect can be avoided. It is known that circular convolution in time domain results in multiplication in frequency domain when the channel is stationary so that the received signal $Y(k)$ in frequency domain is the product of transmitted data $X(k)$ and channel response $H(k)$ in the k th subcarrier. Thus, the orthogonality is maintained (if $h(n,m)$ is fixed within the symbol length, then $h(n,m) = h(m)$ is not about time) and data can be easily recovered by

one-tap channel equalizer, i.e., dividing $Y(k)$ by the corresponding $H(k)$.

$$Y(k) = H(k) * X(k) + N(k) \quad (4.1.3.1)$$

$Y(k)$, $X(k)$, $H(k)$, $N(k)$ are the k th subcarrier after DFT according to $y(i)$, $x(i)$, $h(i)$, $n(i)$. About that we can know the channel is flat fading at each subcarrier.

4.2 MIMO-OFDM Architecture

According to Section 4.1, OFDM technique turns frequency-selective fading channel into several flat-fading subchannels, and it solves the major problem in wideband transmission systems. We will employ V-BLAST technique to detect the transmitted signals on each subcarrier of a MIMO-OFDM systems. MIMO-OFDM transceiver and receiver architectures are shown in Figures 4.5 and 4.6 respectively. Subchannels are orthogonal to each other in OFDM systems. Hence, in single-input-single-output (SISO) OFDM systems, the received signals are product of channel response and transmitted signal. In MIMO systems, signals transmitted from different antennas on a subcarrier simultaneously interfere each other, but signals at different subcarriers are independent. At each receiver antenna, a linear combination of the transmitted signal and channel response on each subcarrier is observed. That corresponds to assumptions of MIMO systems. On each subchannel, a space division multiplexing (SDM) is similar to V-BLAST is applied. That is, the task is to recover x from the received signal y and channel state information (CSI) \mathbf{H} on each subcarrier.

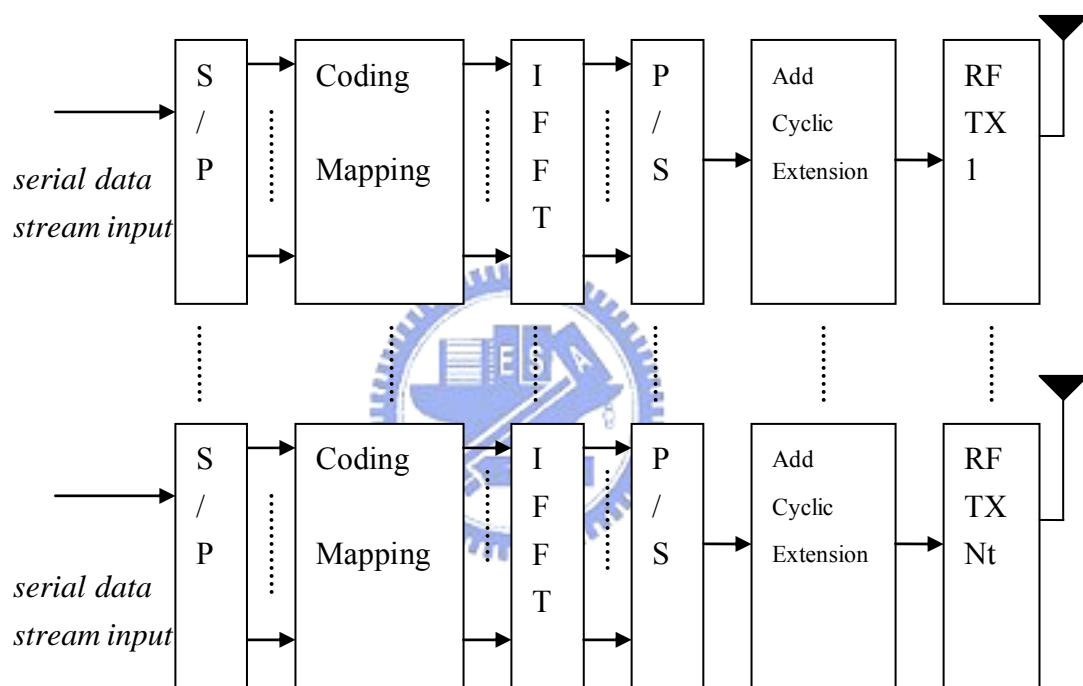


Figure 4-6 Transmitter architecture of MIMO OFDM systems

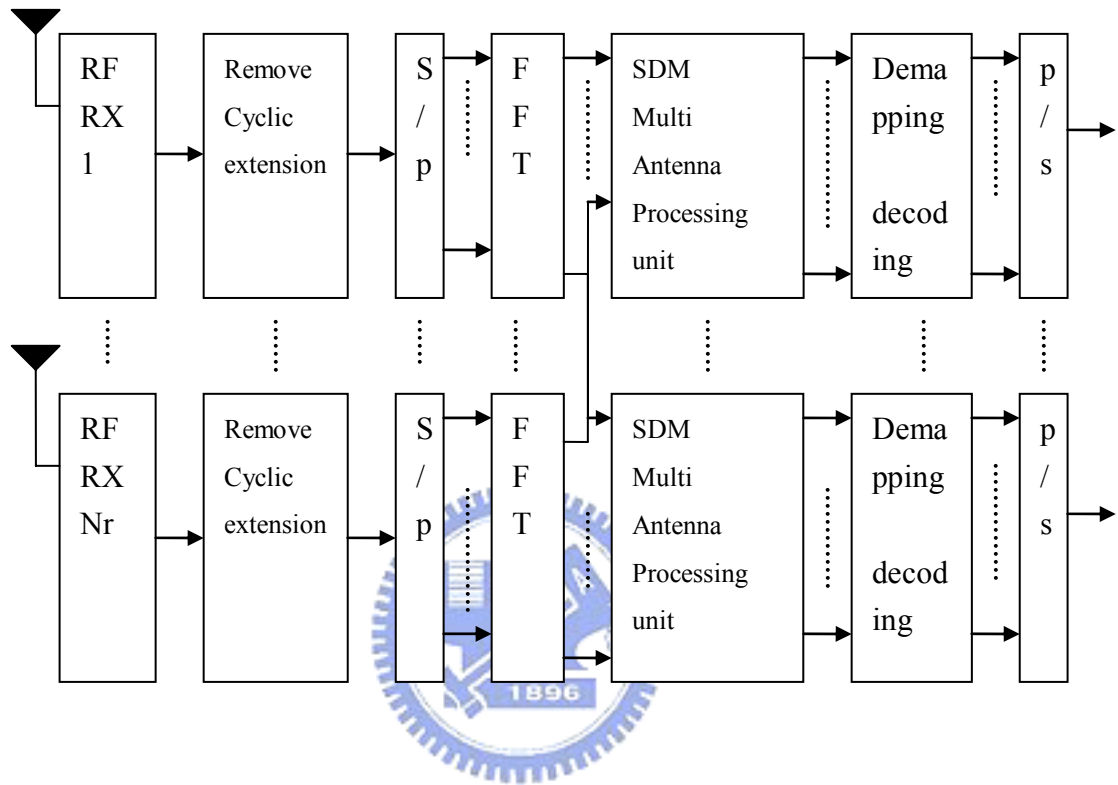


Figure 4-7 Receiver architecture of MIMO OFDM systems

4.3 B-Chase Detector in MIMO-OFDM Systems

We will employ MIMO-OFDM systems to extend the B-Chase detector in the MIMO systems. Due to OFDM systems can turn frequency-selective fading channel into several flat-fading subchannels and get high spectral efficiency. When the channel state is multipath

and the cyclic prefix length is longer than the path delay, we can use flat fading MIMO case to handle it in each subcarrier which do not interfere other subcarriers. That is robust for the frequency-selective fading channel when we detect the received signal in the B-Chase detector. We can say that the frequency-selective fading channel can get time delay diversity when we can handle the frequency-selective fading channel as the flat fading channel. For that we can employ OFDM to get that. The subsequent MIMO signal processing takes place on each subcarrier identically. In order to describe the flat fading MIMO systems observed at each subcarrier in the frequency domain. We let $\mathbf{a}^i = [a_1^i, \dots, a_{N_t}^i]^T$ denote the $N_t \times 1$ transmit signal vector of subcarrier i , then the corresponding $N_r \times 1$ receive signal vector

$\mathbf{r}^i = [r_1^i, \dots, r_{N_r}^i]^T$ is given by



$$\mathbf{r}^i = \mathbf{H}^i \mathbf{a}^i + \mathbf{w}^i \quad (4.3.1)$$

The $N_r \times 1$ dimensional vector $\mathbf{w}^i = [w_1^i, \dots, w_{N_r}^i]^T$ represents independent white Gaussian noise of variance $(\sigma_n^i)^2$ observed at the N_r receive antennas while the average transmit power of each antenna is normalized to one, i.e. $E[(\mathbf{a}^i)(\mathbf{a}^i)^H] = \mathbf{I}_{N_t}$ and

$E[(\mathbf{w}^i)(\mathbf{w}^i)^H] = (\sigma_n^i)^2 \mathbf{I}_{N_r}$. The $N_r \times N_t$ channel matrix \mathbf{H}^i contains uncorrelated complex Gaussian fading gains with unit variance. We assume that the channel matrix \mathbf{H}^i is constant over a frame and changes independently between frames (block fading channel). That in the following the algorithms are given on the base of subcarrier i assuming an outer loop over all subcarrier $i=1, \dots, N_{\text{FFT}}$. The index i is therefore omitted to simplify matters giving $\mathbf{r} = \mathbf{r}^i$, the received signal on subcarrier i , $\mathbf{H} = \mathbf{H}^i$, the channel matrix, $\mathbf{a} = \mathbf{a}^i$, the transmit symbols on

subcarrier i and $\mathbf{w} = \mathbf{w}^i$, the noise vector respectively. From that we detect the transmitted signals on each subcarrier of MIMO-OFDM systems by B-Chase detector.

Table 4-1 System parameters

FFT length	16
Symbol period	16 samples
Cyclic prefix	4 samples
Modulation	16-QAM
Transmit antenna	4
Receive antenna	4
Channel is updated in T symbol periods	8
Rayleigh-fading	Mean=0, Varance=1
Channel order	3
List length ℓ	1 , 2, and 16

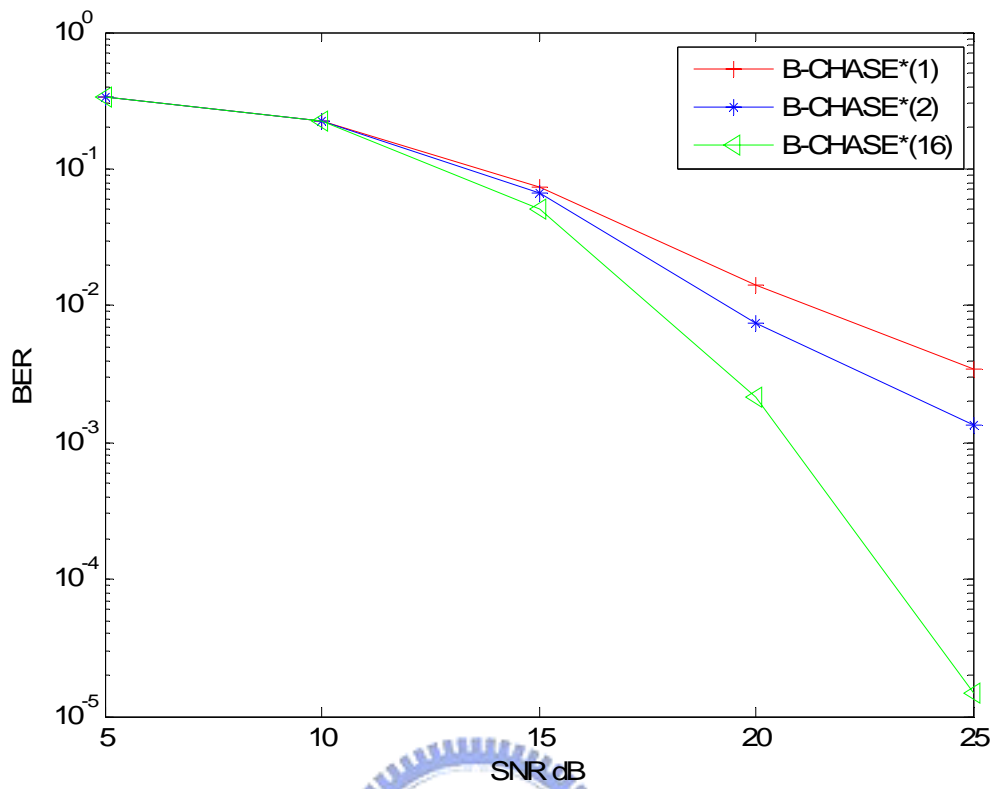


Figure 4-8 Bit error rate versus SNR in the B-Chase detector* (ℓ) with $\ell=1,2,16$ for MIMO-OFDM Systems

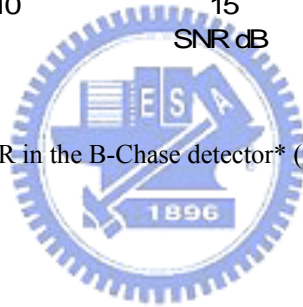


Table 4-2 System parameters

FFT length	16
Symbol period	16 samples
Cyclic prefix	4 samples
Modulation	BPSK
Transmit antenna	4
Receive antenna	4
Channel is updated in T symbol periods	8
Rayleigh-fading	Mean=0, Varance=1
Channel order	3
List length ℓ	1, 2

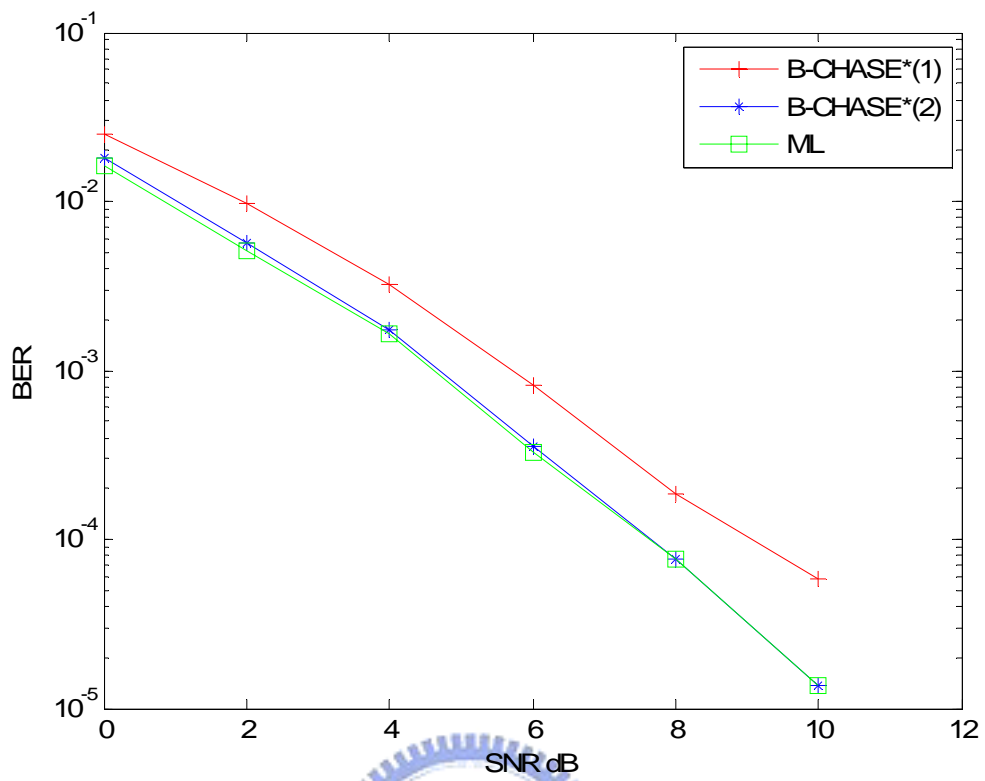
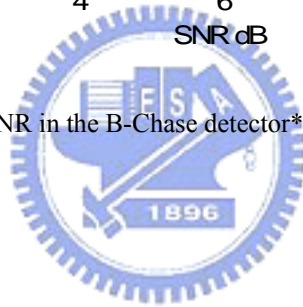


Figure 4-9 Bit error rate versus SNR in the B-Chase detector* (ℓ) with $\ell=1,2$ for MIMO-OFDM Systems



Chapter 5

Conclusion

The B-Chase of detection algorithm is a combination of a list detector and a parallel bank of subdetectors. The B-Chase detector that can trade performance for reduced complexity by modifying the list length. When applying the B-Chase of detection algorithm in the MIMO-OFDM, we can improve performance in the frequency-selective fading channel.



References

- [1] G. J. Foschini, "Layered space-time architecture for wireless communication in a fading environment when using multiple antennas," Bell laboratories Technical Journal, Vol. 1, No. 2, pp. 41-59, 1996.
- [2] P. W. Wolniansky, G. J. Foschini, G. D. Golden, R. A. Valenzuela, "V-BLAST an architecture for realizing very high data rates over the rich-scattering wireless channel," Invited paper; Proc. ISSSE-98, Pisa, Italy, 1998.
- [3] W. J. Choi, R. Negi, and J. Cioffi, "Combined ML and DFE decoding for the V-BLAST system," in *Proc. IEEE Conf. Commun.*, Jun. 2000, pp. 1243–1248.
- [4] D. W. Waters and J. R. Barry, "The chase family of detection algorithms for multiple-input multiple-output channels," in *Proc. GLOBECOM '04*, VOL.4 , Nov. 2004, pp. 2635–2639.
- [5] R. Böhnke, D. Wübben, V. Kühn, and K. Kammeyer, "Reduced complexity MMSE detection for BLAST architectures," in *Proc. IEEE Global Telecommun. Conf. (IEEE GLOBECOM)*, Dec. 2003, vol. 4, pp. 2258–2262.
- [6] D. Wübben, R. Böhnke, J. Rinas, V. Kühn, and K. Kammeyer, "Efficient algorithm for decoding layered space-time codes," *Electron. Lett.*, vol. 37, no. 22, pp. 1348–1350, Oct. 2001.
- [7] D. W. Waters and J. R. Barry, "Noise-predictive decision-feedback detection for multiple-input multiple-output channels," *IEEE Trans. Signal Process.*, vol. 53, no. 5, pp. 1852–1859, May 2005.
- [8] Y. Li and Z. Luo, "Parallel detection for V-BLAST system," in *Proc. IEEE Conf. Commun.*, May 2002, vol. 1, pp. 340–344.
- [9] G.Y. Lin and S.G. Chen, "On signal Detection of MIMO OFDM Systems" Master thesis, Institute of Electronics College of Electrical Engineering, Hsinchu, Taiwan, National Chiao Tung University, 2004.
- [10] Y.C. Chang and S.G. Chen, "Investigation of V-BLAST Detection Technique and Its Improvement for MIMO OFDM Systems " Master thesis, Institute of Electronics College of Electrical Engineering, Hsinchu, Taiwan, National Chiao Tung University, 2006.

- [11] A. Paulraj, R. Nabar, and D. Gore, Introduction to Space-Time Wireless Communications. Cambridge Univ. Press, 2003.
- [12] Clemens Michalke, Hrishikesh Venkataraman, V. Sinha, W. Rave1, and G. Fettweis
“Application of SQRD Algorithm for Efficient MIMO-OFDM Systems.”
http://www.mns.ifn.et.tu-dresden.de/publications/2005/Michalke_C_EW_05.pdf
- [13] D. W. Waters and J. R. Barry, “The chase family of detection algorithms for multiple-input multiple-output channels,” in *Proc. GLOBECOM '08*, VOL.56 , NO.2 Feb. 2008, pp. 739–747.
- [14] A. Chan and I. Lee, “A new reduced-complexity sphere decoder for multiple antenna systems,” in *Proc. IEEE Conf. Commun.*, 2002, pp.460–464.
- [15] G. J. Foschini, G. Golden, R. Valenzuela, and P. Wolniansky, “Simplified processing for wireless communication at high spectral efficiency,” *IEEE J. Sel. Areas Commun.*, vol. 17, no. 11, pp. 1841–1852, Nov. 1999.
- [16] J. Jaldén, L. G. Barbero, B. Ottersten, and J. S. Thompson, “Full diversity detection in MIMO systems with a fixed-complexity sphere decoder,” in *Proc. IEEE Conf. Acoustics, Speech, Signal Processing (ICASSP)*, Apr. 2007, vol. 3, pp. 49–52.
- [17] Deric W. Waters “Signal Detection Strategies and Algorithms for Multiple-Input Multiple-Output Channels”
http://smartech.library.gatech.edu/dspace/bitstream/1853/7514/1/waters_deric_w_200512_phd.pdf
- [18] Vahid Tarokh, Ayman Naguib, Nambi Seshadri, and A. R. Calderbank, “Space-time codes for high data rate wireless communication: Performance criteria in the presence of channel estimation errors, mobility, and multiple paths,” *IEEE Trans. on Communications*, vol. 47, no. 2, pp. 199–, February 1999.
- [19] D. W. Waters and J. R. Barry, ”The Sorted-QR Chase Detector for Multiple-Input Multiple-Output Channels” in *Wireless Communications and Networking Conference*, VOL.1 ,March. 2005, pp. 538–543.

自 傳

方自民，西元 1981 年生於台南市。西元 2004 畢業於台灣國立台北科技大學電子系，之後進入交通大學電子研究所攻讀碩士學位，於 2008 年取得碩士學位。研究方向為無線通訊訊號處理。

